

# Transport of Flexible Molecules in Narrow Confinements

Siddhartha Das and Suman Chakraborty<sup>1</sup>

Department of Mechanical Engineering  
Indian Institute of Technology, Kharagpur  
Kharagpur-721302, India

## ABSTRACT

Dynamical characteristics of flexible polymer molecules in nanoscopic confinements are primarily dictated by the relative values of the confinement length scales with respect to the polymer persistence length. Depending on whether the channel height is larger [1] or smaller [2] than the polymer persistence length, altogether different polymer dynamics is ensued, as illustrated in the pioneering theoretical studies by de Gennes [1] and Odijk [2]. Rapid advances of nanofabrication and polymer handling, over the last few years, have been able to provide experimental validation to these studies and at the same time have been able to unravel different intriguing physical issues unique to nanoconfinement induced dynamics of polymer molecules. These studies have led to a plethora of new applications ranging from the estimation of structural and mechanical properties of polymer to fabrication of novel, portable diagnostic tool kits. In this review article, we shall revisit different physical and technological issues involved in polymer dynamics in nanoconfinements. First, we shall identify the effect of varying degrees of confinement (de Gennes and Odijk regime [1,2]) on the stretching dynamics and the overall representation of the polymer molecule. Next, we shall discuss the possible physical interaction forces on the polymer molecule introduced by the presence of the confining walls and the resulting effects like formation of wall adjacent depletion layers, asymmetric distribution of polymer mass density from the wall to the channel center line etc. Thirdly, we will highlight the possible effects of a background field (flow field or electric field or a combination of both and they may bear signatures of the involved nanoscopic length scales) on the overall nanoscale polymer dynamics. We will also briefly discuss the technological intricacies involved in the relevant nanofabrication and polymer handling schemes and also the issues governing the polymer dynamics modeling involving such scales. Finally, we shall conclude by indicating the possible directions, anticipated outcomes, and significances of future research in polymer transport and dynamics in nanoscopic confinements.

## 1. INTRODUCTION

The present decade has witnessed unprecedented advances in nanofabrication techniques, allowing tremendous developments in sophisticated nanoscale devices that have found enormous applications in virtually every aspects of modern life [3-5]. A number of these applications are based on the analysis of transport of some chemically or biologically significant moieties through these nanoscale devices. The possibilities of interaction of these transported species with nanochannel walls make such analysis extremely intriguing, unraveling a number of fundamental considerations of nanoscale and sub-nanoscale interactions. The complications in the involved analysis are increased manifold in case the transported species are not individual particles, rather polymer molecules which can be viewed as a chain of interconnected macromolecules. A large number of applications covering the wide spectrum ranging from biomedical, pharmaceuticals to forensic investigations that have emerged

---

<sup>1</sup>Corresponding author, e-mail: [suman@mech.iitkgp.ernet.in](mailto:suman@mech.iitkgp.ernet.in)

from the studies of nanoscale transport of a single polymer molecule have motivated the researchers to uptake this extremely challenging task which involves the following sequences of activities: a) design and fabrication of nanochannels of materials that give the desired interaction with the polymer, b) ensuring a smooth passage of the polymer from the immediate surroundings to the nanochannel, c) visualizing the transport and dynamics of the polymer within the nanochannel, d) making the necessary alterations to ensure that the transport is controllable, and finally, e) analyzing the results in the light of the established theories elucidating the effects of confinement on the polymer transport and dynamics.

The present review first revisits the fundamental issues describing the polymer dynamics as a function of the relative value of its radius of gyration with respect to the channel dimensions. We discuss the different modeling strategies like Brownian Dynamics Simulation (BDS), Molecular Dynamics Simulation (MDS) and Monte Carlo (MC) Simulation techniques that are commonly used to capture the behaviour of a confined polymer, as a function of the different intra-molecular and polymer-wall interaction forces. We further elucidate different physical phenomena stemming from such interactions encountered by the polymer molecule, including the issues pertinent to nanochannel transport. Next, we delineate the possible effects of a background flow field, or an externally applied electric field on the transport and dynamics of the nanoconfined polymer. Finally, we outline the possible directions of future research on nanoscale transport of flexible macromolecules.

## 2. EFFECTS OF CONFINEMENT IN ALTERING THE SCALING LAWS

One of the most important analyses pertinent to polymer dynamics analysis is to obtain appropriate scaling relations connecting the different quantities expressing the instantaneous polymer dimensions (like its radius of gyration, end to end distance etc. [1]) with the parameters intrinsic to the polymer (like the number of monomers constituting the polymer,  $N$ ) or the system geometry. For unconfined polymers, the scaling relationships are well known and have been detailed by a number of researchers [1, 6, 7]. The important expressions read:

$$R_g^2 = b^2 \frac{N}{6} \quad (1)$$

(valid for the case when the polymer is modeled as an ideal chain, i.e., the volume exclusion effects [1] are neglected; here  $R_g$  is the radius of gyration of the polymer and  $b$  denotes the random walk distance of the polymer)

and

$$R_f = bN^{3/5} \quad (2)$$

(valid for the case when the polymer is modeled as a real chain, i.e., the volume exclusion effects are included; here  $R_f$  is the end to end distance of the polymer chain)

For cases in which the polymer is forced into the confinement, the channel dimension, in conjunction with number of monomers, dictates the scaling behaviour. In fact, depending on the relative dimension of the channel height ( $H$ ) with respect to the polymer radius of gyration ( $R_G$ ), two distinct regimes may be observed, in which the polymer behaves altogether differently. Typically, for nanoconfined systems, we have  $H < R_G$  (for most of the well-known polymer molecules like DNA,  $R_G \geq 1 \mu m$ ). For such cases, depending on the relative value of the polymer persistence length ( $L_p$ ) with respect to the channel height, two further behavioural regimes have been identified. For cases with  $L_p < H$ , the polymer is said to be de Gennes regime; whereas for  $L_p > H$ , the polymer is in the Odijk regime. In the subsequent sections we provide detailed derivation of the scaling and dynamic response of the polymer in these two regimes.

### 2.1.1 Polymer response in de Gennes regime ( $L_p < H$ )

To derive the scaling behaviour, one first needs to invoke the free energy description of the polymer chain. Assuming it to be a real polymer chain, the free energy is a sum of the contribution from the excluded volume and the chain coiling.

The free energy change due to exclusion volume effect is expressed as:

$$\frac{\Delta A_{ch,EV}}{k_B T} = \frac{v_s (N/n_s)^2}{2R_{CP}^3} \quad (3)$$

where  $R_{CP}$  is the instantaneous value of the polymer end to end distance,  $N$  is the total number of monomers,  $n_s$  is the number of monomers per spring/rod (typically the polymer is assumed to have a bead-rod or bead-spring configuration [1]),  $N/n_s$  is the total number of springs/rods in the system,  $v_s$  is the excluded volume per spring/rod,  $k_B$  is the Boltzmann constant and  $T$  is the absolute temperature. The free energy change due to chain coiling may be expressed as:

$$\frac{\Delta A_{ch,C}}{k_B T} = \frac{3R_{CP}^2}{2R_{0R}^2} \quad (4)$$

where  $R_{0R} = \sqrt{2Na_m L_P}$  is the random walk radius and  $a_m$  is the length of a monomer.

For confinement dimensions satisfying the following:  $R_g > H > L_p$ , the polymer having an instantaneous end-to-end distance of  $R_{CP}$  may be assumed, according to de Gennes blob model [1], to be conceived as a series of  $K = R_{CP}/D_{Sp}$  nonpenetrating spheres with radius  $D_{Sp}/2$  (here  $D_{Sp} = H$ ) and  $N/K$  monomers (see Fig. 1). According to de Gennes, each sphere may be described by the Flory theory (i.e., total free energy of each type is obtained by multiplying number of spheres,  $K$ , with the free energy corresponding to segment present in each sphere). Thus, the total free energy becomes:

$$\frac{\Delta A_{ch}(R_{CP})}{k_B T} = K \frac{\Delta A_{ch,Sp}}{k_B T} \quad (5)$$

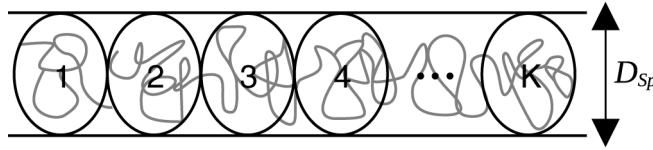


Figure 1. de Gennes "Blob" model of confined polymer in a channel of diameter  $D_{Sp}$  ( $= H$ ) describing the molecule as a series of  $K$  self-avoiding spheres (for  $R_g > H > L_p$ ).

where  $\Delta A_{ch,Sp}$  is the free energy change of the polymer segment associated with each sphere. For the excluded volume contributions, one may write:

$$\Delta A_{ch,EV,Sp} = \frac{v_s (N/Kn)^2}{2(D_{Sp}/2)^3} = \frac{4v_s N^2}{n_s^2 D_{Sp}^3 K^2} \quad (6)$$

Similarly, for the chain coiling contribution, one gets:

$$\Delta A_{ch,C,Sp} = \frac{3(D_{Sp}/2)^2}{2R_{0R,Sp}^2} = \frac{3D_{Sp}^2}{8\{2(N/K)a_m L_P\}} = \frac{3KD_{Sp}^2}{8\{2Na_m L_P\}} = \frac{3KD_{Sp}^2}{8R_{0R}^2} \quad (7)$$

Using Eqs. (6) and (7) in Eq. (5), along with the condition  $K = R_{CP}/D_{Sp}$ , one gets:

$$\frac{\Delta A_{ch}(R_{CP})}{k_B T} = \frac{4v_s N^2}{n_s^2 D_{Sp}^2 R_{CP}} + \frac{3R_{CP}^2}{8R_{0R}^2} \quad (8)$$

This total free energy is minimized to obtain the equilibrium Flory radius, as:

$$\left[ \frac{\partial}{\partial R} \left( \frac{A_{ch}}{k_B T} \right) \right]_{R_{CP}=R_f} = 0 \Rightarrow R_f = \left( \frac{32v_s a_m L_P}{3n_s^2 D_{Sp}^2} \right)^{1/3} N \quad (9)$$

In all the above considerations,  $D_{Sp} = H$ , consistent with the extent of occupancy of the polymer.

### 2.1.2 Polymer response in Odijk regime ( $L_p > H$ )

In this case, as explained by Odijk [2], the coiling behaviour of the polymer is altogether lost and the polymer acts as a combination of several rigid segments that are “reflected” by the hard walls of the channel (See Fig 2). Accordingly, the polymer dynamics may be discussed in terms of the instantaneous radius and tangent vectors of the rod-like polymer structures [2].

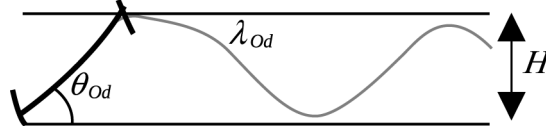


Figure 2. Deflected segments characterized by the length scale  $\lambda_{Od}$  for a polymer in Odijk regime (for  $H < L_p$ ).

First, one may consider an unconfined worm-like polymer chain described by the radius vector  $\mathbf{r}_p(t_c)$  as a function of the contour distance  $t_c$  from one end to that point. A tangential unit vector is defined as:

$$\mathbf{u}_p(t_c) = \frac{\partial \mathbf{r}_p(t_c)}{\partial t_c} \quad (10)$$

$$\mathbf{u}_p^2(t_c) = 1 \quad (11)$$

and  $\mathbf{u}_p(0)$  is a point along the z-axis of the Cartesian coordinate system (x,y,z). The statistics of the chain are derived using the free energy of curvature as:

$$\frac{\Delta A_{ch}}{k_B T} = \frac{1}{2} L_p \int_0^L \left( \frac{\partial \mathbf{u}_p}{\partial t_c} \right)^2 dt_c \quad (12)$$

Different averages of the WLC near the rigid rod limit may be obtained as:

$$\langle \mathbf{r}_p^2(t_c) \rangle = t_c^2 \left[ 1 - \frac{t_c}{3L_p} + O\left(\frac{t_c^2}{L_p^2}\right) \right] \quad (13)$$

$$\langle (\mathbf{r}_p(t_c) \cdot \mathbf{u}_p(t_c))^2 \rangle = \langle z_p^2(t_c) \rangle = t_c^2 \left[ 1 - \frac{t_c}{L_p} + O\left(\frac{t_c^2}{L_p^2}\right) \right] \quad (14)$$

Using Eqs. (13) and (14), one may derive the mean square average deviation away from the z-axis due to thermal fluctuations, as:

$$\langle \boldsymbol{\varepsilon}_p^2(t_c) \rangle = \langle x_p^2(t_c) + y_p^2(t_c) \rangle = 2 \langle x_p^2(t_c) \rangle = \frac{2t_c^3}{3L_p} \quad (15)$$

The above expression is valid as long as  $t_c$  is less than  $L_p$ .

Now, this polymer chain is assumed to be inserted in a very narrow (height  $D_{Sp} \ll L_p$ ; in the subsequent analysis we write  $H$  in place of  $D_{Sp}$ ), long pore, with the pore's central axis being placed along z axis of the chain. It is also assumed that the chain does not interact with the pore except for hard wall repulsions at the pore surface. Under these circumstances, one may state in an approximate sense that the average mean square deviation  $\boldsymbol{\varepsilon}_p^2(t_c)$  varies as  $\left(\frac{H}{2}\right)^2$ , and for that one may replace the contour distance  $t_c$  with a newly introduced length scale  $\lambda_{Od}$ , so as to obtain (neglecting coefficients):

$$\begin{aligned} \langle \varepsilon_p^2(\lambda_{Od}) \rangle &\sim (H/2)^2 \sim \frac{2\lambda_{Od}^3}{3L_p} \\ \Rightarrow \lambda_{Od} &\sim (H^2 L_p)^{1/3} \end{aligned} \quad (16)$$

Thus, for a polymer of contour length  $L_c$ , it is plausible to replace the chain within the pore by a sequence of  $L_c/\lambda_{Od}$  links each of length  $\lambda_{Od}$  (See Fig. 2).

The instantaneous end to end distance ( $R_{CP}$ ) is the number of Odijk segments ( $L_c/\lambda_{Od}$ ) times the average projection of an Odijk segment on the channel axis. Hence,

$$R_{CP} = \left( \frac{L_c}{\lambda_{Od}} \right) \{ \lambda_{Od} \cos(\theta_{Od}) \} = L_c \cos(\langle \theta_{Od} \rangle) \quad (17)$$

where  $\langle \theta_{Od} \rangle$  is the average deflection made by the polymer with the walls. Assuming  $\langle \theta_{Od} \rangle$  to be sufficiently small (so that  $\cos(\langle \theta_{Od} \rangle) \approx 1 - \frac{1}{2} \langle \theta_{Od} \rangle^2 = 1 - \frac{1}{2} \left( \frac{H}{\lambda_{Od}} \right)^2 = 1 - \frac{1}{2} \left( \frac{H}{L_p} \right)^{2/3}$ ) one may get from Eq. (17):

$$R_{CP} = L_c \left[ 1 - A_{Od} \left( \frac{H}{L_p} \right)^{2/3} \right] \quad (18)$$

where  $A_{Od}$  is a numerical constant that may appear (as the scaling laws were originally derived neglecting coefficients), which is calculated as 0.361 [2].

Assuming the total polymer length to be divided into  $L_c/\lambda_{Od}$  Odijk segments, one may describe the change in confinement free energy as:

$$\Delta A_{Conf} = k_B T \frac{L_c}{\lambda_{Od}} = k_B T \frac{L_c}{H^{2/3} L_p^{1/3}} \quad (19)$$

On eliminating  $H$  from Eqs. (18) and (19), a closed form expression for the free energy is obtained in terms of the end to end distance  $R_{CP}$ , i.e.,

$$\Delta A_{Conf} = k_B T \frac{L_c A_{Od}}{L_p (1 - R_{CP}/L_c)} \quad (20)$$

Differentiating the free energy expression twice with respect to  $R_{CP}$ , one may get the equivalent spring constant as:

$$k_{Od} = 2k_B T \frac{A_{Od}}{L_p L_c (1 - R_{CP}/L_c)^3} \quad (21)$$

Using Eq. (18) in Eq. (21), and neglecting the numerical coefficients, one gets:

$$k_{Od} \simeq \frac{k_B T}{L_c} \frac{L_p}{H^2} \quad (22)$$

In the Odijk limit, the friction arises primarily from the hydrodynamic interaction of a polymer segment with the channel wall. The wall-polymer interactions lead to a friction factor  $\xi_{Od}$  given as [8,9]

$$\xi_{Od} \cong \frac{2\pi\eta L_c}{\ln(H/w_p)} \quad (23)$$

where  $L_c$  is the polymer contour length,  $w_p$  is the width of the polymer molecule and  $\eta$  is the dynamic viscosity of the solvent in which the polymer is placed in the nanochannel. Using Eqs. (22) and (23), one may finally obtain the time scale  $\tau_{Od}$  for the Odijk regime as (neglecting coefficients):

$$\tau_{Od} = \frac{\xi_{Od}}{k_{Od}} \cong \frac{\eta L_c^2}{k_B T L_p} \frac{H^2}{\ln(H/w_p)} \quad (24)$$

## 2.2 Experimental evidences of the validation of the scaling laws

With the tremendous advances in the nanofabrication technologies and the knowledge to handle single polymer molecules in thin nanochannels, researchers have been able to experimentally investigate the validity of the different scaling laws pertaining to the nanoconfined polymer. Tegenfeldt et al. [10] were among the first to study the dynamics of a nanoconfined DNA molecules (in a 100 nm channel) and observed that the stretching behaviour is in well agreement with the scaling predictions of de Gennes theory. Reisner et al. [11] in his study observed the expansion of a nanoconfined DNA and found that the results showed remarkably good agreement in the Odijk regime, but had some deviation in the de Gennes regime [11]. Reccius et al. [12], in their work, drove initially compressed (electrophoretically) DNA molecules into nanochannels and the resulting confinement-induced expansion were explained by a model that is a variation of de Gennes's polymer model. Lin et al. [13] investigated DNA dynamics in photolithography-manufactured nanochannels using fluorescence microscopy to confirm the scaling predictions of de Gennes for the end to end distance and radius of gyration of a nanoconfined polymer. Cross et al. [14] investigated the DNA mobility in a 19 nm slit nanochannel and observed the DNA response to be not totally in Odijk regime, but somewhat in between the sub-blob (de Gennes [1]) and the rigid rod (Odijk regime [2]) regimes. Such transitional behaviour was also noted by other researchers [11,12,15]. Bonthuis et al. [16] used fluorescence microscopy to study the shape and dynamics of individual DNA molecules in de Gennes and Odijk regimes. Radius of gyration and the relaxation time were found to follow the predicted scaling in the de Gennes regime. Unexpectedly, in the Odijk regime the relaxation time showed a sharp decrease and the radius of gyration remained constant. The possible explanations to such anomalous behaviour in the Odijk regime can be attributed to the likely existence of a number of other scaling regimes in between the de Gennes and the Odijk regimes, as recently established by Odijk [17]. Thanmdrup et al. [18] studied the stretching of DNA in polymer nanochannels designed by fast and inexpensive technique of nanoimprint lithography in PMMA and obtained good agreement with de Gennes predictions. In a very recent study, Park et al. [19] devised a novel method for the fabrication of nanochannels required for DNA molecule stretching. The nanochannels were fabricated by a combination of reactive ion etching of silicon, which controls the dimension of the final structure, and simple deformation of polydimethylsiloxane (PDMS) films onto the fabricated structure. Their results of DNA stretching are in well agreement with the scaling predictions of Odijk.

## 2.3. Studies exploring other possible scaling behaviour of a nanoconfined polymer

Other than the above described simple scaling laws, explaining the equilibrium properties of a nanoconfined polymer in de Gennes and Odijk regimes, other scaling relationships (either derived from the standard de Gennes or Odijk model, or completely deviated from these two models) also describe a nanoconfined polymer molecule. In a very early study, Chen and Muthukumar [20] used path integral representation of Edwards to study the free energy of a confined chain and obtained the identical scaling prediction of the de Gennes model. Wagner et al. [21] in their study went beyond the standard model of a nanoconfined polymer (i.e., within Odijk or de Gennes regimes) and gave exact quantitative description of the square of the end to end distance of a polymer chain ( $\langle R^2 \rangle$ ) in the Weakly Bending Regime for strong confinements (Odijk regime), as:

$$\frac{\langle R^2 \rangle_c}{L_c^2} = 1 - \frac{\varepsilon_p}{2c_{Od}} \left\{ 1 + \frac{1}{c_{Od}^2} \left[ 1 - \sqrt{2} e^{-c_{Od}} \sin \left( c_{Od} + \frac{\pi}{4} \right) \right] \right\} \quad (24a)$$

where  $L_c$  is the contour length,  $c_{Od} = L_c / \lambda_{Od}$  and  $\varepsilon_p = L_c / L_{Od}$ . Yang et al. [22] used a simulation algorithm similar to the pruned enriched Rosenbluth method to give exact quantification of the coefficient  $A_{Od}$  (see Eq. 18) appearing in the scaling description of the end to end distance of the

polymer confined in the Odijk regime. They also obtained the equivalent scaling coefficients for a channel with rectangular cross section. Arnold et al. [23] used Monte Carlo simulation to show that the scaling estimate for relaxation time ( $\tau$ ), as predicted by de Gennes blob model ( $\tau \sim N^2 D^{1/3}$ ;  $D$  being the nanochannel height), fails for small to moderate values of  $N$  ( $N \leq 2000$ ) and is only valid in the regime  $N \gg D^{5/3} \gg 1$ . Sakae [24] obtained the scaling relationships for semi flexible polymer chains and illustrated how the complications due to the consideration of additional length scale arising from the chain rigidity results in more diverse behaviors, as compared to the case with flexible polymers (Odijk and de Gennes regimes), depending on system parameters. In an all new different study, Klushin et al. [25] proposed a scaling estimate for a flexible polymer chain slowly dragged by one end of a nanotube of diameter ( $D$ ) in the de Gennes regime. They demonstrated that when the chain end is dragged by a certain critical distance  $x^*$  into the tube, the polymer chain exhibits a first order phase transition resulting in the remaining free tail to be abruptly sucked into the tube. This critical distance scales as  $x^* \sim ND^{1-1/\nu}$ , where  $\nu$  is the Flory's exponent.

### 3. INTERACTION FORCES ON NANOCONFINED POLYMER AND THE DIFFERENT MODELING STRATEGIES

One of the key areas of research on nanoconfined polymer transport is to devise the appropriate modeling strategies that correctly predict the polymer dynamics by accounting for the different interactions encountered by the polymer in presence of confinement. The continuum based free energy approach, as adapted in the previous section to describe the scaling behaviour, may not always be satisfactory to explain the consequences of different forces encountered by a polymer in close proximity of the nanochannel walls and one may need to invoke molecular simulation methods (like MDS) or coupled molecular-continuum simulation method (like BDS or MC). The most popular and well practiced method to study dynamics of confined polymer has been BDS. In this method the polymer is typically represented as a bead-spring or a bead-rod model and the motion of each bead is studied by assuming it to be obeying Newton's laws of motion. Such Lagrangian description of the beads allows including the different interaction forces that they experience from the walls, the solvent and the adjacent as well as the non-adjacent beads. However, the solvent is described by a continuum Eulerian representation with an additional modification that accounts for the effect of Hydrodynamic Interaction (HI). In the following sections we detail the Brownian Simulation methodology for capturing polymer dynamics in a nanochannel and in the process highlight the cause and the significances of the different continuum and non-continuum interaction forces that the beads experience from the nanochannel walls. We also elucidate the possible advantages and disadvantages in a similar study addressed by MDS and other standard simulation techniques.

#### 3.1 Brownian dynamics simulation of nanoconfined polymer: consideration of different polymer-wall interaction forces

Let us consider a flexible polymer molecule, dissolved in the viscous solvent, enclosed in a slitlike nanochannel. The polymer may be represented by an equivalent bead-spring model, with  $N_b$  numbers of beads being connected through  $N_s = (N_b - 1)$  numbers of entropic springs. Brownian Dynamics Simulation strategies allow this chain to be represented by the stochastic differential equation [26-29]:

$$d\mathbf{r} = \left[ \mathbf{V} + \frac{\mathbf{D} \cdot \mathbf{f}}{k_B T} + \frac{\partial}{\partial \mathbf{r}} \cdot \mathbf{D} \right] dt + \sqrt{2} \mathbf{B} \cdot d\mathbf{w} \quad (25)$$

$$\mathbf{D} = \mathbf{B} \cdot \mathbf{B}^T \quad (26)$$

In eq. (25),  $\mathbf{r}$  is a vector containing  $3N_b$  spatial coordinates of the beads constituting the polymer chain,  $\mathbf{f}$  is a vector of length  $3N_b$  denoting the non-Brownian non-hydrodynamic forces acting on each bead (the different wall induced interaction forces on the beads are included in  $\mathbf{f}$ ) and  $\mathbf{V}$  is a vector of length  $3N_b$  representing the unperturbed fluid velocity field at the location of the bead.  $3N_b$  components of  $d\mathbf{w}$  may be obtained from a real-valued Gaussian distribution having mean zero

and variance  $dt$ . The movement of each segment of the chain disturbs the unperturbed background velocity field (this velocity field can be a pure pressure-driven one, or an electroosmotic one, or a combination of both), which in turn affects the motion of the entire polymer, as manifested through HI. These interactions may be represented by a  $3N_b \times 3N_b$  diffusion tensor, expressed as [26-29]

$$\mathbf{D}_{ij} = k_B T \left[ (6\pi\eta R_b)^{-1} \mathbf{I} \delta_{ij} + \mathcal{Q}_{ij} \right] \quad (27)$$

where  $R_b$  is the bead hydrodynamic radius, and  $\mathcal{Q}_{ij}$  is the HI tensor that relates the velocity perturbation at a position  $\mathbf{r}_i$  due to a point force exerted at  $\mathbf{r}_j$ . The Brownian forces, which appear in the last term of eq. (25), are related to these velocity perturbations through the fluctuation-dissipation theorem [30] (Fixman, 1986). When the polymer is in a confinement, the HI tensor is a linear combination of the interaction tensor in an infinite domain and the interaction tensor representing the correction that accounts for the constraints imposed by the confining walls. Thus  $\mathcal{Q}_{ij}$  can be expressed as [26-28]

$$\mathcal{Q}_{ij} = \mathcal{Q}^w(\mathbf{r}_i, \mathbf{r}_j) + (1 - \delta_{ij}) \mathcal{Q}^{OB}(\mathbf{r}_i - \mathbf{r}_j) \quad (28)$$

where  $\mathcal{Q}^{OB}$  is the free space Green's function (or Oseen-Burgers tensor), and  $\mathcal{Q}^w$  is a correction that accounts for wall-induced hydrodynamics. In Brownian dynamics simulations of polymers [26], one usually replaces  $\mathcal{Q}^{OB}$  by the Rotne-Prager-Yamakawa (RPY) tensor  $\mathcal{Q}^{RPY}$ , expressed as

$$\begin{aligned} \mathcal{Q}^{RPY}(\mathbf{r}_i - \mathbf{r}_j) &= \frac{1}{8\pi\eta|\mathbf{r}_i - \mathbf{r}_j|} \left[ C_1 \mathbf{I} + C_2 \frac{(\mathbf{r}_i - \mathbf{r}_j)(\mathbf{r}_i - \mathbf{r}_j)}{|\mathbf{r}_i - \mathbf{r}_j|^2} \right] & \text{if } |\mathbf{r}_i - \mathbf{r}_j| \geq 2R_b \\ &= \frac{1}{6\pi\eta R_b} \left[ C'_1 \mathbf{I} + C'_2 \frac{(\mathbf{r}_i - \mathbf{r}_j)(\mathbf{r}_i - \mathbf{r}_j)}{|\mathbf{r}_i - \mathbf{r}_j|^2} \right] & \text{if } |\mathbf{r}_i - \mathbf{r}_j| < 2R_b \end{aligned} \quad (29)$$

where

$$C_1 = 1 + \frac{2R_b^2}{3|\mathbf{r}_i - \mathbf{r}_j|^2}, \quad C_2 = 1 - \frac{2R_b^2}{|\mathbf{r}_i - \mathbf{r}_j|^2}, \quad C'_1 = 1 - 9\frac{|\mathbf{r}_i - \mathbf{r}_j|}{32R_b}, \quad C'_2 = \frac{3|\mathbf{r}_i - \mathbf{r}_j|}{32R_b} \quad (30)$$

To retain the symmetric positive-semidefiniteness of  $\mathbf{D}$  despite this replacement,  $\mathcal{Q}_{ij}^w$  may be modified as

$$\mathcal{Q}_{ij}^w = 0.5 \left( \mathcal{Q}_{ij}^w + \mathcal{Q}_{ji}^{wT} \right) \quad (31)$$

The wall HI tensor  $\mathcal{Q}^w$  is such that the velocity perturbation it creates due to a point force  $\mathbf{f}(\mathbf{x}_j)$  located at a point  $\mathbf{x}_j$  is

$$\mathbf{v}_w'(\mathbf{x}, \mathbf{x}_j) = \mathcal{Q}^w(\mathbf{x}, \mathbf{x}_j) \cdot \mathbf{f}(\mathbf{x}_j) \quad (32)$$

This perturbation may be obtained by solving the following boundary value problem (this boundary value problem assumes that the flow field is a combination of the pressure-driven and electroosmotic transport [31]):

$$-\nabla p + \eta \nabla^2 \mathbf{v}_w' + \left( e \sum_N z_i n_i \right) \mathbf{E} = 0, \quad \nabla \cdot \mathbf{v}_w' = 0 \quad (33)$$

subject to

$$\left( \mathbf{v}_{RPY}' + \mathbf{v}_w' \right)_{wall} = 0 \quad (34)$$

The  $i$ -th column of  $\mathcal{Q}^w(\mathbf{x}, \mathbf{x}_j)$  may accordingly be evaluated as:

$$\begin{bmatrix} \Omega_{1i}^w & \Omega_{2i}^w & \Omega_{3i}^w \end{bmatrix}^T = \frac{1}{f_i} \mathbf{v}'_w \quad (35)$$

where  $f_i$  is a point force acting along  $x_i$  and located at  $x_i$ .

The non-hydrodynamic and non-Brownian force  $\mathbf{f}$  appearing in eq. (25) accounts for all other interaction effects encountered by the beads. These effects can be broadly classified into three types: a) interaction forces from the other beads (or portion of the chain), b) forces arising from the bead-wall interaction and c) forces arising from the interaction of the beads with an established/induced field in the nanochannel. The bead-bead interactions are composed of inter-bead spring force, force arising from the finite rigidity of the chain, bead-bead dispersion-repulsion interaction force captured by standard Lennard Jones (LJ) potential and mutual Columbic electrostatic interaction force between the charged beads. The spring force between the adjacent beads may be modeled using WLC (Worm-like Chain) approximation, such that [26]

$$\mathbf{f}_{ij}^S = \frac{k_B T}{2b_k} \left[ \left( 1 - \frac{|\mathbf{r}_i - \mathbf{r}_j|}{q_0} \right)^{-2} - 1 + 4 \frac{|\mathbf{r}_i - \mathbf{r}_j|}{q_0} \right] \frac{\mathbf{r}_i - \mathbf{r}_j}{|\mathbf{r}_i - \mathbf{r}_j|} \quad (36)$$

Here  $\mathbf{f}_{ij}^S$  represents the spring force exerted on the bead  $i$  by the bead  $j$ ,  $b_k$  is the Kuhn length of the polymer chain,  $q_0$  is the maximum extension of the molecule (expressed as  $q_0 = N_{k,s} b_k$ , with  $N_{k,s}$  being the number of Kuhn segments per spring). The finite rigidity of the chain may be accounted by appealing to the harmonic bending potential between the adjacent beads [32] expressed as:

$$U_{i,i+1}^{bend} = 0.5k_s \left\{ \arccos(\hat{\mathbf{b}}_i \cdot \hat{\mathbf{b}}_{i+1}) \right\}^2 \quad (37)$$

where  $\hat{\mathbf{b}}_i = \frac{\mathbf{r}_{i+1} - \mathbf{r}_i}{|\mathbf{r}_{i+1} - \mathbf{r}_i|}$ , and  $k_s$  is the constant of rigidity. The bead-bead dispersion-repulsion force may

be characterized by standard LJ interaction, expressed as

$$\begin{aligned} \mathbf{f}_{ij}^{LJ} &= 4\epsilon_{LJ,b} \left[ \frac{12\sigma_{LJ,b}^{12}}{|\mathbf{r}_i - \mathbf{r}_j|^{13}} - \frac{6\sigma_{LJ,b}^6}{|\mathbf{r}_i - \mathbf{r}_j|^7} \right] \frac{\mathbf{r}_i - \mathbf{r}_j}{|\mathbf{r}_i - \mathbf{r}_j|} \quad \text{for } |\mathbf{r}_i - \mathbf{r}_j| \leq 2^{1/6} \sigma_{LJ,b} \\ &= 0 \quad \text{for } |\mathbf{r}_i - \mathbf{r}_j| > 2^{1/6} \sigma_{LJ,b} \end{aligned} \quad (38)$$

where  $\epsilon_{LJ,b}$  and  $\sigma_{LJ,b}$  are LJ parameters corresponding to the beads.

Most of the polymers have finite electrical charge. This charge is assumed to be distributed equally among the different beads. In an ionic solution the charges on the beads are neutralized by counterions, resulting in the formation of an Electric Double Layer [33] surrounding the bead. Under such conditions, the inter-bead Columbic electrostatic potential for bead 'i' may be expressed as [34]:

$$\mathbf{f}_c = - \sum_{\substack{j \\ j \neq i}} \frac{q_b^2 l_B k_B T}{\lambda^2} \exp\left(-\frac{|\mathbf{r}_i - \mathbf{r}_j|}{\lambda}\right) \frac{\mathbf{r}_i - \mathbf{r}_j}{|\mathbf{r}_i - \mathbf{r}_j|} \quad (39)$$

where  $q_b$  is the charge on the bead,  $\lambda$  is the EDL thickness and  $l_B = e^2/4\pi\epsilon k_B T$  is the Bjerrum length (state the physical significance of the Bjerrum length).

The bead wall interaction forces are combinations of different continuum (like bead-wall Double Layer interaction, van der Waals interaction etc.) and non-continuum (like Steric interaction, solvation interaction, Straining interaction etc.) effects. Accordingly, we can write:

$$\mathbf{f}_{wall} = \mathbf{f}_{DL} + \mathbf{f}_{vdW} + \mathbf{f}_{Steric} + \mathbf{f}_{solv} + \mathbf{f}_{Strain} \quad (40)$$

In Eq. (40), is the force experienced by each bead as a result of the interaction of the EDLs of the bead with the channel walls, and may be expressed as [35,36]:

$$f_{DL} = \left\{ \frac{\frac{32\varepsilon_0\varepsilon_r R_b \left(\frac{k_B T}{e}\right)^2 \tanh\left(\frac{e\zeta}{4k_B T}\right) \tanh\left(\frac{e\zeta_b}{4k_B T}\right)}{\lambda \left[1 - \frac{\frac{2R_b + 1}{\left(\frac{R_b}{\lambda} + 1\right)^2} \tanh^2\left(\frac{e\zeta_b}{4k_B T}\right)}{\lambda}\right]^{\frac{1}{2}}} \left[ \exp\left(-\frac{h_s}{\lambda}\right) - \exp\left(-\frac{2H - 2R_b - h_s}{\lambda}\right) \right] \right\} \mathbf{j} \quad (41)$$

where  $\zeta_b$  is the zeta potential of the bead surface,  $2H$  is the channel height and  $h_s$  is the separation distance of the bead from the channel bottom wall. Similarly in Eq. (40),  $f_{vdW}$  is the van der Waals (vdW) force of interaction between the beads and the channel walls, expressed as [35,36]:

$$f_{vdW} = \left\{ \begin{aligned} & \frac{A}{6} \frac{\bar{\lambda}\bar{s}}{(\bar{\lambda} + \bar{s}h_s)^2} \left[ \ln\left(\frac{h_s + 2R_b}{h_s}\right) - \frac{2R_b}{h_s} \frac{h_s + R_b}{h_s + 2R_b} \right] - A \left( \frac{\bar{\lambda}}{\bar{\lambda} + \bar{s}h_s} \right) \frac{2R_b^3}{3h_s^2 (h_s + 2R_b)^2} \\ & - \frac{A}{6} \frac{\bar{\lambda}\bar{s}}{\{\bar{\lambda} + \bar{s}(2H - 2R_b - h_s)\}^2} \left[ \ln\left(\frac{2H - h_s}{2H - 2R_b - h_s}\right) - \frac{2R_b}{2H - 2R_b - h_s} \frac{2H - R_b - h_s}{2H - h_s} \right] \\ & + A \left( \frac{\bar{\lambda}}{\bar{\lambda} + \bar{s}(2H - 2R_b - h_s)} \right) \frac{2R_b^3}{3(2H - 2R_b - h_s)^2 (2H - h_s)^2} \end{aligned} \right\} \mathbf{j} \quad (42)$$

where  $A$  is the Hamaker constant for interaction between the bead and the wall with an intervening liquid medium,  $\bar{\lambda}$  is the ‘London characteristic wavelength’ (here taken as 100 nm), and  $\bar{s}$  is a constant (here taken as 11.116). Figure 3 demonstrates the possible magnitudes of these two continuum bead wall interaction forces as a function of the separation distance for different values of bead radii. For separation distances of the order of nanometers, these effects are found to be extremely large (the signs of the different forces imply that the vdW effect imparts a wall-directed attractive push on the polymer beads, whereas the DL interaction imparts a repulsive push on the beads away from the wall), indicating large impact of these two forces in nanochannel transport of finite sized moieties [31,37,38]. Also these two effects demonstrate opposite dependences on bead radii sizes.

Other than the continuum effects mentioned above, there can be non-continuum interaction forces active between the nanochannel wall and the polymer. For such non-continuum effects, the structure and the distribution of the water molecules around the beads and the nanochannel wall become the key dictating factors. One can identify three such non-continuum bead-wall interactions, namely, *Solvation Interaction*, *Straining Interaction* and *Steric Interaction*. For all these interactions, the pertinent length scales typically vary from few nanometers to angstroms, implying that these effects can be influential in extremely narrow nanoconfinements.

*Solvation Interaction* typically refers to the forces that are associated with the formation/disruption of solvent layers around solid substances, like a flat wall, a macromolecule or even a small ion [39] (Israelachvili, 2003). When a solid body is introduced in a liquid, the liquid molecules adjacent to the surface rearrange to pack well against it, as this helps to lower the overall free energy. Such ordering does not require any liquid-liquid or liquid-wall interactions, rather is solely determined by the geometry of the molecules and how they pack around the constraining boundaries. When one solid

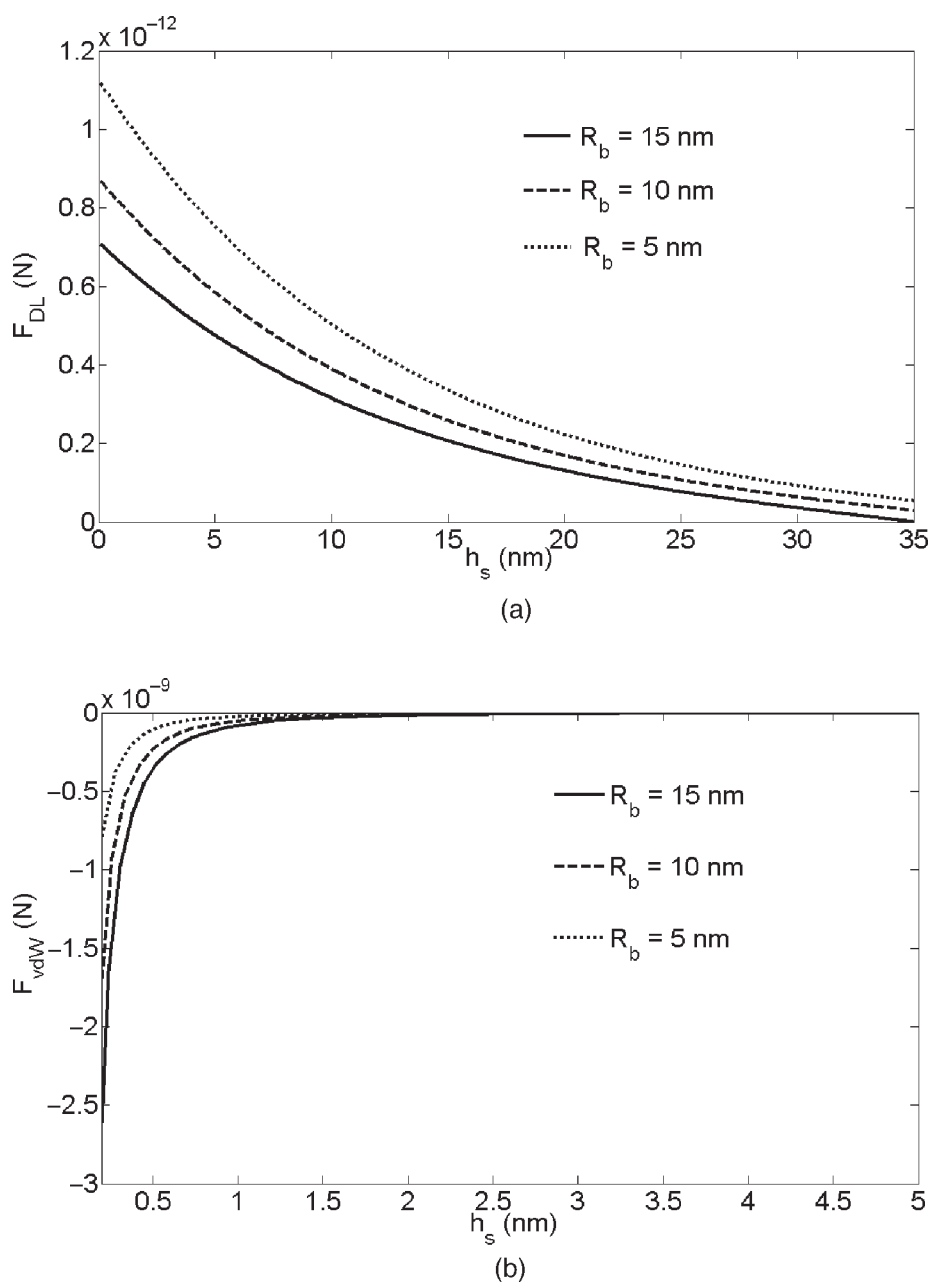


Figure 3. Variation of (a) DL and (b) vdW interaction forces with separation distance from the channel bottom wall (the picture depicts the variation only in the channel bottom half) for different values of bead radii (taking  $A = 10^{-20}$  J,  $H/\lambda = 4$ ,  $T = 300$  K,  $H = 50$  nm).

surface is brought in the vicinity of another one, the ordering of the solvent molecules is disrupted and they rearrange to find the most energetically favourable packing geometry. It takes energy to disrupt the original ordering of the liquid. Thus, the presence of the second surface generates an oscillatory solvation pressure (which may be attractive or repulsive) as a function of the separation distance between the two surfaces. In case the interacting surfaces are atomically smooth (e.g. mica surfaces), the solvation interaction becomes a monotonically decaying function of the separation distance [39]. The characteristic length scale ( $l$ ) over which the solvation forces become active is typically of the order

of few nanometers and may be expressed in terms of the bead-bottom wall separation distance  $h_s$ , as [40] (Majumdar and Mezic, 1998)

$$f_{solv} = U_{solv} \left( \frac{l_s}{h_s^2} + \frac{1}{l_s} + \frac{1}{h_s} \right) \exp\left(-\frac{h_s}{l_s}\right) - U_{solv} \left( \frac{l_s}{(2H-h_s)^2} + \frac{1}{l_s} + \frac{1}{2H-h_s} \right) \exp\left(-\frac{2H-h_s}{l_s}\right) \quad (43)$$

where  $U_{solv}$  is the solvation interaction energy and  $l_s$  is the solvation decay length. Figure 4 depicts the variation of the solvation interaction forces with the separation distance for different values of the solvation decay length. The force is found to decay very rapidly with distance (within a span of few nanometers only), indicating the effectiveness of this force only in very thin nanochannels. Increase in solvation decay length increases the range of effect of the solvation interaction, and consequently increase in solvation decay length increases the magnitude of the interaction for a given separation distance (see fig. 4).

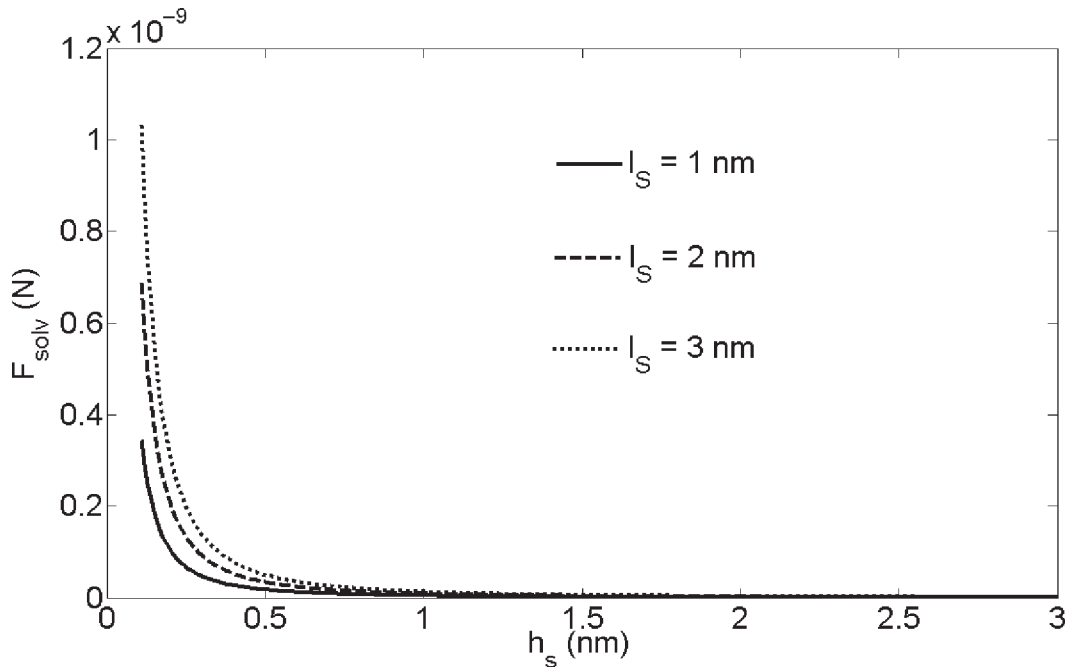


Figure 4. Variation of solvation interaction forces with separation distance from the channel bottom wall (the picture depicts the variation only in the channel bottom half) for different values of solvation decay length (taking,  $U_{solv} = k_B T$ ,  $T = 300$  K,  $H = 50$  nm).

Other than solvation interaction, straining and steric interactions can also be significant in largely reduced non-continuum systems. Layering of the solvent molecules in the vicinity of a solid substrate means that this liquid layer exhibits a solid-like behaviour with a particular lattice constant. If this constant is not equal to that of the solid substrate, then the bonds between the solvent molecules in the solvation-induced layered structure may be strained. The interaction energy resulting from such straining may be mathematically approximated as [40]

$$f_{Strain} = -\frac{E_e \epsilon_0^2}{2} \left[ \exp\left(-\frac{h_s}{l}\right) - \exp\left(-\frac{2H-h_s}{l}\right) \right] \quad (44)$$

where  $E_e$  is the elastic modulus the solid phase of the liquid (which may be heterogeneously nucleated to form a solid-like layered structure adhering to the substrate) and  $e_0$  is the strain in the first monolayer (typically ranging between 0 to 5%).

*Steric effects* originate as a result of repulsive interactions between the electron clouds of two molecules, preventing them from occupying identical location in space at a particular time. The bead-wall Steric repulsion force may be described as [32]

$$\mathbf{f}_{Steric} = -\frac{5l_0^2 k_B T}{(|y_i| - H)^3} \mathbf{j} \quad (45)$$

where  $y_i$  is the transverse coordinate of the bead and  $l_0$  is the equilibrium bond length. In a very recent study, Das et al. [31] have elucidated the possible effects of these different interaction forces on the dynamics of a nanoconfined polymer.

There can be forces on the polymer beads due to some established fields (these fields can be particularly strong for nanoconfinement) within the channel. For example, the EDL field established within the channel can impart transverse electrophoretic force on the charged polymer beads, resulting in a net EDL force as [31]:

$$\mathbf{f}_{ep} = 6\pi\eta R_b \left[ \mu_{ep} (E_{ext} + E_I) \mathbf{i} - \mu_{ep} \frac{d\psi}{dy} \mathbf{j} \right] \quad (46)$$

In Eq. (46),  $\mu_{ep}$  is the electrophoretic mobility of the polymer beads,  $\psi$  is the EDL potential field.

Further,  $-\frac{d\psi}{dy} \mathbf{j}$  is the transverse EDL field and  $\mathbf{f}_{ep} = -(6\pi\eta R_b) \mu_{ep} \frac{d\psi}{dy} \mathbf{j}$  is the transverse electrophoretic

force (for a nanoconfined system  $\frac{d\psi}{dy}$  can be significantly large ensuring a strong enough transverse electrophoretic effect that can significantly affect the transport of finite size moieties [37,38]),  $E_{ext}$  is the externally applied electric field (if any), and  $E_I$  is the induced electric field (which can be typically a streaming electric field that is generated from the pressure-driven transport of an ionic liquid [33,41]). Effects of streaming field on nanoconfined polymer transport are discussed in details in Section 5.4.

Another external field that can be important for nanoconfined polymer transport may originate due to thermophoretic migration of polymer beads caused by viscous dissipation induced appreciable local temperature gradients prevailing in the nanofluidic systems. By integrating the Smoluchowski equation, a thermodynamically consistent expression for the resultant thermal (Soret) diffusion coefficient ( $D_T$ ) may be obtained in the following form [42]

$$D_T = D_0 \frac{\rho_b}{T} \left[ \alpha_T \phi_b + O(\phi_b^2) \right] \quad (47)$$

where  $\rho_b$  is the number density of the polymer beads,  $T$  is the absolute temperature (which varies in the system, due to viscous dissipation),  $\phi_b$  is the bead volume fraction,  $D_0 = \frac{k_B T}{6\pi\eta R_b}$ , and  $\alpha_T$  is a leading-order virial coefficient [42]. The consequent thermophoretic transport is accounted for by incorporating

an additional forcing term  $\frac{1}{\rho_b} (-D_T \nabla T) dt$  in the stochastic equation of motion of the polymer chain (eq. 25).

On the basis of identical considerations,  $D_{ij}$  may also be modified to account for thermal gradients prevailing in the system, by multiplying the same with the correction factor [42],  $\left[ 1 + \alpha_m \phi_b + O(\phi_b^2) \right]$

where  $\alpha_m$  is a leading order virial coefficient. Possible implications of Soret effect in nanoconfined polymer transport have been reported in a number of recent studies [31,43].

Detailed Brownian dynamics studies on nanoconfined polymer transport have been reported consistently in the literature over the last few years. In one of the earliest studies, Tian and Smith [44] used BDS to study the translocation of a polymer through a nanopore in presence of a driving chemical potential gradient. Another very early work was by Wang and Gao [45], who used Brownian simulation to observe the dynamics of a strongly confined semiflexible polymer in presence of hydrodynamic interactions. Hernández-Ortiz et al. [46] used BDS to study the nanoconfined flowing polymer solutions and pinpointed the effects of concentration on hydrodynamically induced migration phenomena. Chen et al. [47] gave a comparative estimate between the use of Lattice Boltzmann method and BDS in modeling DNA in strong confinements. They found that the former method is well-suited for long polymer chains as well as semidilute and concentrated DNA solutions, whereas Brownian dynamics is better to capture dilute DNA solutions. Huopaniemi et al. [48] investigated polymer translocation through a nanopore in presence of an external force by Langevin dynamics. In a similar study, Wei et al. [49] used Langevin dynamics simulation to study the unforced polymer translocation through a nanopore in an impermeable membrane. Luo et al. [50] used Langevin dynamics to study the influence of attractive polymer-wall interactions on the nanopore translocation of a polymer, and found that there is a substantial alteration in total translocation time. They also investigated, through Langevin dynamics, the possible effects of sequence dependence on the nanopore translocation of the DNA molecules [51]. Mobius et al. [52] used a combination of BDS and a coarse-grained stochastic model to study the dynamics of a knot in a semiflexible polymer confined to a narrow channel of width comparable to the polymers' persistence length. Huang and Marakov [53] used Langevin dynamics to study the rate constant of polymer reversal inside a nanopore. Prinsen et al. [54], in an extremely interesting study, considered a polymer to be partially confined in a nanotube and calculated the resulting force acting on the confined polymer portion.

### 3.2 Molecular dynamics simulation (MDS) of nanoconfined polymer transport

In nanoconfinements, it may often happen that the involved length scales become small enough so that it is no longer possible to model the solvent implicitly, as is done in case of Brownian simulations. For such cases, each of the involved species (the different polymer beads, all the water molecules and all the wall atoms) is modeled explicitly, i.e., for each of them we solve Newtonian force equations. Primary advantage of such explicit modeling for a nanoconfined system is that it helps to avoid accounting of the different polymer-wall and polymer-solvent interaction forces (very often incorporation of such forces requires a detailed understanding of the physical system, which may not be known *a priori*). Typically, there are two types of interactions between the different species. The first one is the short-ranged LJ interaction between all the involved atoms (the energy and length scales get altered depending on the nature of the interacting species) and the long-ranged Coulombic interactions between the different charged species (for instance, one may have charges on the polymer beads, nanochannel wall atoms as well as the oxygen atom on the water molecule). Through a comprehensive accounting of these forces, the kinematics of each of the species can be evaluated. Consequently, different macroscopic properties of interest, such as the polymer chain density distribution, average speed of the polymer translocation in the confinement, etc. can be obtained.

Rapid advancements in computational facilities have allowed researchers to extensively use explicit molecular simulations for studying dynamics of nanoconfined polymer molecules. One of the earliest contributions was by Kuppa and Manias [55], who used MDS to study the dynamics of poly (ethylene oxide) in nanoconfinements. Schwartz et al. [56] investigated the  $\alpha$ -relaxation and normal relaxation processes in the dynamics of nanoconfined oligomeric poly (propylene glycol) (PPG) liquids of different molecular weights using molecular simulations. For a single DNA molecule in an ionic solution, the behaviour of the surrounding cations and counterions become critically important to dictate the DNA dynamics. However, in quasi-continuum methods like the Brownian simulation, the presence of the counterions and cations is grossly summarized by considering that they lead to the formation of an EDL and consequently, all the electrostatic interactions get screened by the effective Debye Layer thickness. The fact that these ions are not individually addressed may lead to a number of oversimplified conclusions. Overcoming such barriers, Rabin and Tanaka [57] carried out a full scale

molecular simulation of the equilibrium ionic distribution in the vicinity of a single DNA molecule in a nanopore. They showed that in the presence of DNA, the counterions condense on the stretched macromolecule, thereby effectively neutralizing the same. They further demonstrated that there is nearly complete depletion of coions from the pore. Other notable molecular simulation studies of ionic distribution around a nanoconfined polymer include those by Aksimentiev et al. [58], Lau et al. [59], Cui [60], Heng et al. [61], Luan and Aksimentiev [62] etc.

Molecular simulation can be further used to accurately predict different equilibrium properties of a nanoconfined polymer. For example, Arnold et al. [23] used a combined MC and Molecular Dynamics technique to obtain the relaxation time for a self-avoiding polymer chain confined in a cylindrical nanopore. Dimitrov et al. [63] used molecular simulations to investigate the correctness of scaling predictions of the different universal properties of a polymer molecule confined in a nanoslit. Höfling et al. [64] used MDS to prove the scaling relations from the quick transverse equilibration to the slowest process of orientational relaxation in a very long nanochannel. Jung et al. [65] performed molecular simulations to study the elastic and dynamic behavior of a self-avoiding chain confined inside a cylindrical nanopore. They pinpointed the possible effects of including hydrodynamic interactions in altering the scaling exponents governing the relaxation time. MDS has also been used to explore a number of intriguing physical phenomena, never known before, associated with the dynamics of a nanoconfined polymer. Matysiak et al. [66] used MDS to draw important inferences (not predicted by scaling theories) for a nanoconfined polymer. They found two distinct translocation regimes, depending on the ratio of pore and polymer length. In addition, they categorized the translocation velocity and time as a function of the externally applied voltages and temperatures. Khare et al. [43] used MDS to investigate the cross-stream migration of polymer in a nanochannel under equilibrium condition as well as pressure-driven transport. They also investigated the possible effects of a thermal gradient on the transverse variation of the polymer chain density. Melchionna et al. [67] used a multiscale simulation technique (molecular dynamics for polymer bead motion and Lattice Boltzmann method for solvent motion) to demonstrate that translocation of a long biopolymer in a nanopore (large enough to accommodate multiple polymer strands) proceeds through multifolded configurations characterized by a well-defined integer number of folds. As a result, the passage time is a function of the average folding number, causing a deviation from the single-exponent power law characterizing single-file translocation through narrow pores. Gauthier and Slater [68] used all atom MDS to reveal that during the polymer translocation through a nanopore, the escape and the relaxation processes are coupled. Strikingly enough, the last half of the chain was found to escape from the nanopore in less than 12% of the total escape time. Fyta et al. [69] employed multiscale simulation (combined Lattice Boltzmann- Molecular Dynamics) to establish that the coupling of the correlated molecular motion with hydrodynamics results in significant acceleration of the translocation of a nanoconfined polymer. Luan and Aksimentiev [62] carried out all atom MDS to identify the possible causes of the force experienced by DNA in a bulk electrolyte confined in a solid-state nanopore when subject to an external electric field.

### 3.3 Other simulation techniques for studying transport of nanoconfined polymers

Other than Brownian Dynamics and Molecular dynamics, simulation techniques such as Monte Carlo (MC), Lattice Boltzmann (LB), Density Functional Theory (DFT), Dissipative Particle Dynamics (DPD) etc. that have been used to study the transport and dynamics of a nanoconfined polymer. Procedural details of these different techniques are well documented in the literature and we avoid those in this review. Rather, we cite the different references in which these techniques have been successfully used to capture the confinement induced response of a polymer molecule. In one of the very early contributions, Wang and Teraoka [70] employed lattice MC simulation technique to investigate the thermodynamics and structures of linear chain molecules between parallel plate confinements for different values of polymer concentration. This group published a number of other papers on MC simulation of confined polymers. [71-75] Bundschuh and Gerland [76] used kinetic MC method to demonstrate that during nanopore translocation of DNA and RNA, there may occur transient formation of base pairs which may significantly hasten up the translocation. Cacciuto and Luijten [77] applied

MC method to show that the translocation time during the escape of a self-avoiding polymer chain from a nanopore exhibited a nonlinear dependence on the degree of polymerization, with a strong sensitivity to the nature of the confining geometry. Among the very recent studies involving MC simulations are the investigations of dragging a polymer chain into a nanotube and its subsequent release by Klushin et al. [25], corroborating a correlation between the structure and dynamics of a nanoconfined polymer chain by Kalb and Chakraborty [78], measurement of the conformational response of a supercoiled DNA to nanoconfinements by Lim et al. [79], tracking the polymer as a single Brownian particle diffusing in presence of external driving forces and the internal entropic bias by Gauthier and Slater [80], measurement of the rotation time of the end-to-end vector of the polymer, the diffusion time for the center of the polymer and the looping time for the ends of the polymer in presence of nanoconfinements of different geometries by Cui et al. [81], calculation of different dynamic scaling exponents for nanopore polymer translocation by Luo et al. [82] etc.

Other than MC techniques, methods like LB, DPD etc. have also been used to study nanoconfined polymers. As have been already pointed out, several investigations with coupled MDS and LB methods have been executed to accurately capture the nanoconfined polymer dynamics in the least possible computational time [67,69]. There are also examples where LB method is used alone to capture the polymer transport. For example, Usta et al. [83] used LB method to study the polymer dynamics in periodic and confined geometries. They employed the same LB approach to investigate the possible flow field effects in confinements [84] and transverse migration of a nanoconfined polymer in presence of an external force [85]. Other notable works involving LB simulation of polymers in confinements include those by Reboux et al. [86], Chen et al. [47], Xie et al. [87] etc.

There have also been reports of studying nanoconfined polymer dynamics by methods like DPD and DFT. For example, in a recent study Fedosov et al. [88] employed DPD to study the molecular migration in nanochannels and calculated the thickness of the depletion layers. Millan et al. [89] employed a general framework of DPD to investigate the effects of molecular weight, polymer concentration, and flow rate on the variation of polymer density and velocity across a channel section in pressure-driven transport of a nano-confined polymer solution. In a subsequent work [90], they used the same DPD approach to study the trend of cross-stream migration of the polymer chains in presence nanoscale Poiseuille flow. In a very recent study, Moeendarbary et al. [91] investigated electrophoretic migration of DNA molecules through narrow constrictions using DPD. Ye et al. [92] employed DFT approach to obtain the density and chain conformation profiles of square-well chains confined in nanoslits. Using the same approach they also studied the dynamics of homopolymer [93] and copolymer chains [94] confined in nanoslits.

#### 4. NON-SCALING RESPONSES OF A POLYMER TO NANOCONFINEMENT

When a polymer is forced into a nanoconfinement, a number of physical issues pertaining to the polymer, other than its equilibrium stretching behaviour, become important. These effects may not obey a universal scaling dependence (as a function of the nanochannel height and the polymer properties) as the equilibrium stretching behaviour, but are equally important to describe the effects of confinement on the dynamics of a polymer molecule. We discuss some of these effects along with the notable investigations on them subsequently.

##### 4.1 Polymer chain distribution and depletion layer formation in nanochannels

One major property of confined polymers that has received intense attention for over almost half a century is their entropic depletion near inert hard surfaces due to steric exclusion effects, leading to an attraction force, popularly known as depletion interaction [95-96] (Figure 5 illustrates the possible variations of the depletion interaction force for different combinations of the interaction moieties in different intervening media). This interaction has been successfully used to drive aggregation of colloidal particles [97-99], bacteria [100] and cells [101,102]. Studying the polymer distribution and the resulting depletion interaction in a confinement dates back to the contribution of Oosawa and Asakura more than half a century ago [95]. Since then, a number of researchers [103-107] have enriched the understanding of the polymer distribution and the depletion force in

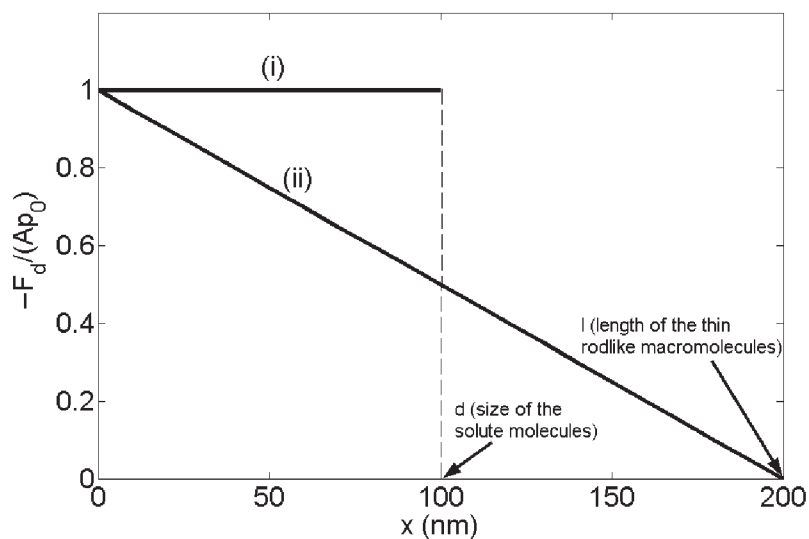


Figure 5a. Depletion interaction force ( $F_d$ ) between two parallel plates in a solution of (i) spherical (of size  $d = 100$  nm) and (ii) rod like macromolecules (of length  $l = 200$  nm). (In this figure  $p_0$  denotes the osmotic pressure of the medium expressed as  $p_0 = k_B TN/V$ , where  $N$  denotes the number of macromolecules and  $V$  denotes the volume of the solution,  $A$  is the area of the parallel plates,  $x$  is the distance between the two plates)

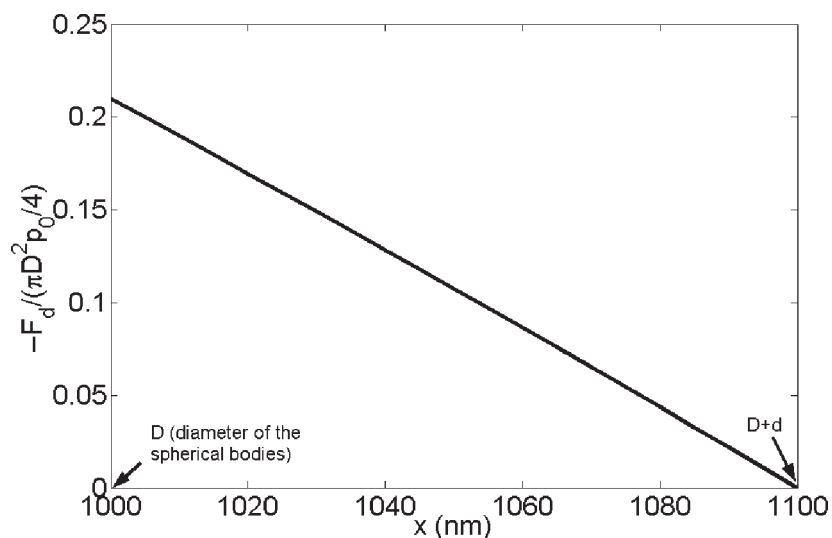


Figure 5b. Depletion interaction force ( $F_d$ ) between two spherical bodies (of diameter  $D = 1000$  nm) in a solution of spherical macromolecules (of diameter  $d = 100$  nm).

confinements of varying dimensions. (Figure 6 demonstrates the chain distribution for pores of varying dimensions).

With the recent developments of applications based on nanoscale transport of polymer molecules, there have been renewed interests in studying the polymer distribution and the depletion layer formation in nanofluidic transport. Eisenriegler and Maassen [108] investigated the center-of-mass distribution of a polymer near a hard repulsive wall. Hsu and Grassberger [109] used Monte Carlo simulation to study the distribution of a three dimensional polymer chain in a confined space. They

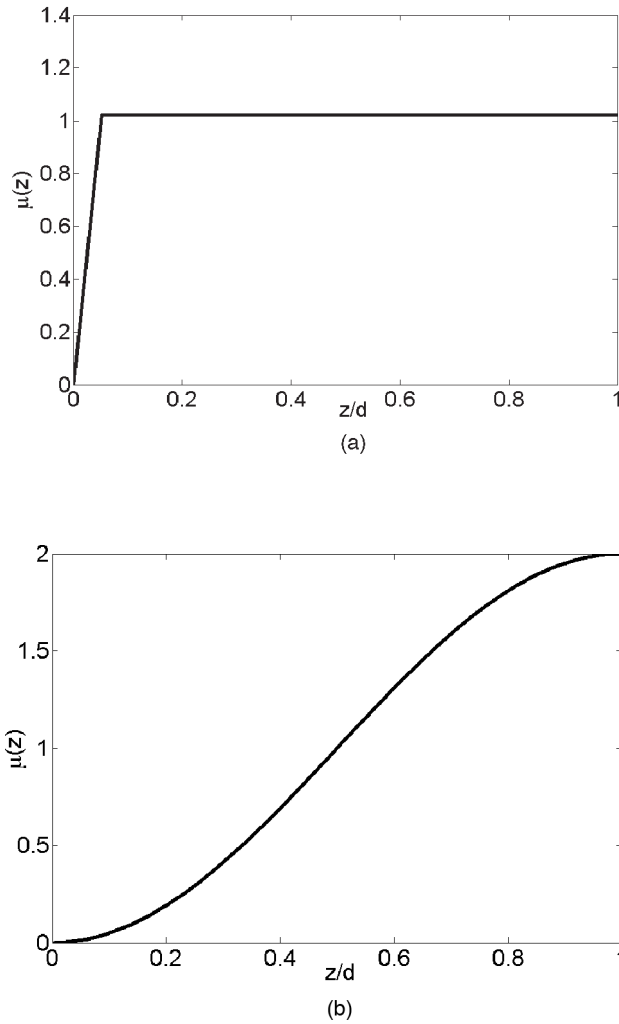


Figure 6. Profiles of macromolecular chain unit distribution (denoted by  $\mu$ ) inside (a) a wide ( $R_g/d = 0.02$ ;  $d$  being the pore radius) and (b) a narrow pore ( $R_g/d = 2$ ) at no adsorption (the distribution is shown in a pore section in between the wall and the centerline). (In this figure  $d$  denotes the radius of the pore,  $z$  denotes the transverse location within the pore and  $R_g$  denotes the radius of gyration of the chain).

The profiles are calculated using the following formulae [103]:

$$1. \quad \mu(z) = K^{-1} \left\{ \begin{array}{l} 1 + \frac{8}{\sqrt{\pi}} [\exp(-\zeta^2) - \exp(-4\zeta^2)] - \\ -2(1+2\zeta^2) \operatorname{erfc}(\zeta) + (1+8\zeta^2) \operatorname{erfc}(2\zeta) \end{array} \right\} \quad (\text{for wide pores})$$

$$2. \quad \mu(z) = 2 \sin^2 \left( \frac{\pi z}{2d} \right) \quad (\text{for narrow pores})$$

$$(\text{where } \zeta = z/2R_g, \quad K = 1 - \frac{2}{\sqrt{\pi}} \frac{R_g}{d}).$$

allowed the channel height ( $D$ ) to vary widely from  $D \gg R_F$  to  $D \ll R_F$  (where  $R_F$  is the Flory radius). In another study, Chen [110] carried out off-lattice MC simulations to study the response of chain molecules confined in a long cylindrical nanopore under the condition of hard-body interaction. It was seen that the chains that are very near the pore surface tend to wrap around the surface in various configurations. Also, the monomer concentration near the pore surface was found to increase with increasing surface curvature. Ye et al. [92,93] employed DFT to investigate the density distribution of a polymer chain introduced in a nanoconfinement having both attractive and repulsive walls. They established that with a decrease in temperature (i.e., decreasing the “goodness” of the solvent), the segment-segment attraction increases, resulting in a stronger depletion of the chain density close to the walls. They also delineated the possible consequences of the chain packing fraction on the extent of near-wall chain depletion [92]. They even explicated the alteration in the chain density profiles in case the polymer changes from a homopolymer to a copolymer [93,94]. They demonstrated that increase in the chain length makes the configurational entropy effect predominant due to the significant intra-segment correlations, leading to enhanced near-wall depletion [93]. Usta et al. [83,84] used LB simulation to predict the mass distribution of a 16-monomer confined polymer in a nanoslit. It was found that in absence of a flow field, the depletion was much thinner as compared to the case with flow, thereby ensuring that the density distribution was more uniformly spread across the channel for the no flow case. The enhanced wall-repelling migration of the polymer (causing this enhanced depletion layer) with background flow was attributed due to the combined effect of hydrodynamic interactions between the pairs of monomers and hydrodynamic interactions between a monomer and a wall [83]. This is in sharp contrast to what happens in the absence of hydrodynamic interactions, where the presence of the flow field stretches the polymer chain by the high shear rate near the wall, enabling the center of mass to access regions closer to the boundary causing a decrease in the depletion layer thickness. Similar influences of flow field, in presence of HI, were predicted for somewhat larger polymer by the MDS study of Khare et al. [43] and BDS study of Hernández-Ortiz et al. [111] and Das et al. [31]. On similar lines, Usta et al. [85], Butler et al. [112], Millan et al. [89] demonstrated that a polymer confined to a narrow channel migrates towards the center when driven by an external force (which may be also due to the presence of a flow field) parallel to the channel walls, caused by the asymmetric hydrodynamic interactions between polymer segments and the confining walls. In a recent work, Wang et al. [113] presented a new method, known as CABS (in this method they defined a new computational method and a new molecular size parameter, referred to as *Steric Exclusion Radius*  $R_s$ ) that allowed easy calculation of equilibrium partition coefficient (and hence the depletion interaction force exerted by the macromolecules) as a function of confinement sizes for different types of confinement. They extended this method to obtain the depletion thickness profiles of confined dilute polymer solutions and established that the depletion layer thickness remains independent of the reference point used to describe the depletion profile [114].

The depletion layer and the resulting polymer mass distribution in confined systems get largely altered in case the walls are adsorbing, as discussed in the large number of publications by Casassa [115-117]. In a recent study, Kleshchanok et al. [118] was able to directly measure the depletion interaction forces between different objects, like two parallel plates, a plate and a sphere, two spheres, etc., and pinpointed the possible differences in the interactions for alteration in the nature of the surface quality from non-adsorbing to adsorbing ones. Sikorski and Żukowska [119] investigated the chain center of mass density profiles across an adsorbing nanoslit for different number of polymer chains. Other noteworthy examples of investigations that delineate polymer chain distribution in adsorbing nanoslits include those by Jaeckel and Dayantis [120], Chen and Escobedo [121], Romiszowski and Sikorski [122-125] etc.

It can be clearly inferred from the above examples that the conditions prevailing at the nanochannel walls largely dictate the polymer chain distribution in the channel. Khare et al. [43] employed MDS to demonstrate the possible variations in the chain density distribution in case the two walls are maintained at two different temperatures. They found that the chain distribution got skewed (showed larger values) towards the wall maintained at a higher temperature, caused by a preferred migration of the polymer molecules towards higher temperature due to Soret effect. This result has further been

supported by the recent Brownian dynamics simulation study of Das et al. [31]. He and coworkers [126, 127] demonstrated by using MDS the possible effects of nanoscale surface features on the nanorheology of the liquid crystalline polymer in nanochannel transport.

#### 4.2 Other non-scalable variations of properties of nanoconfined polymer

Other than alterations in scalable properties like stretching behaviour, diffusivities and non-scalable features like formation of depletion layer, forcing a polymer in a confinement can lead to a number of very intriguing physical phenomena at equilibrium, depending on the nature of the confinement and the polymer, as well as the characteristics of the channel walls. Mishra and Kumar [128] used their model developed for unconfined systems [129, 130], to delineate the role of confinement in altering the equilibrium thermodynamic properties (coil-to-globule transition) of a polymer chain. It was found that with the increase in the degree of confinement, the end-to-end distance of the polymer chain (a measure of the extent of collapse or degree of globule formation) first decreased rapidly and then beyond a certain channel height weakly increased. Maury-Evertsz et al. [131] employed MC simulations to establish that for nanoconfined polymers, coil-to-globule transition resembles the gas to liquid transition and the liquidlike to solidlike transition. They found that the coil-to-globule transition temperature shifted to lower values as the slit width approached the two-dimensional cases (wall separation equal to bead diameter), and to higher values for larger chain lengths. Feng and Fredrickson [132] obtained inhomogeneous properties of equilibrium nanoconfined polymers with numerical self-consistent field theory. They characterized the polymer length distribution as a function of the plate separation distance. Lim et al. [79] used MC simulation to study the nanoconfinement induced conformational behaviour of supercoiled DNA molecules. They demonstrated that with an enhanced extent of the confinement, the supercoil becomes more tightly interwound and long-range structural features such as branching and the formation of hairpins are progressively reduced. Jo et al. [133] demonstrated that disposable devices featuring both micro- and nanoscale features can successfully elongate DNA molecules when buffer conditions are controlled to alter DNA stiffness, thereby paving the way for manufacturing of nanoscale DNA barcoding systems. Some other related studies exploring dynamics and non-scalable properties of nanoconfined polymer include the investigations on the formation of micro-phases in a melt of asymmetric block copolymers confined in thin nanoslits [134], field theoretic simulation of confined polymer solutions elucidating the role of monomer excluded volume and concentrations on the chemical potential and chain distribution across the nanochannel [135, 136], formation of well-developed microphase separated structures of block copolymers in cylindrical nanoconfinements [137, 138], surface-induced phase transitions in ultrathin films of block copolymers [139], confinement induced crystallization of cylindrical diblock copolymers [140] phase segregation of diblock copolymers in nanopore geometries [141], formation of confinement-induced novel morphologies by block copolymers [142] etc.

### 5. EXTERNAL EFFECTS DRIVEN TRANSPORT OF NANOCONFINED POLYMER

Over the years, one of the greatest challenges encountered by the research community has been to controllably drive a charged polymer through nanoconfinements. This stems from the fact that the passage of a polymer molecule through a narrow confinement involves a large entropic barrier and demands the application of a driving force. An external effect in the form of a directly subjected force, or an electric field (exploiting the charged nature of a polyelectrolyte), or an established flow field have been among the most effective methods to provide this force so as to move a polymer molecule through nanochannels. In the subsequent sections, we will focus on some of the significant research achievements on these aspects.

#### 5.1 Transport of nanoconfined polymer in presence of electrical forces

The charged nature of DNA and similar other polymer molecules renders the technique of manipulation of nanoconfined polymer molecules by applying external electric fields very popular. Assuming that the effective charge of a DNA base pair ( $q_{eff}$ ) is represented as a function of the position along the polymer

contour (i.e.,  $q_{eff} = q_{eff}(s)$ ), one can calculate the net electrical force ( $F_{el}$ ) on the polymer molecule due to an externally applied position dependent electric field  $E(s)$  as:

$$F_{el} = \int \left[ \frac{q_{eff}(s)}{a_p} \right] E(s) ds \quad (48)$$

where  $a_p$  is the distance between two base pairs, and the integral is taken along the DNA contour length.

Efforts to drive a polymer through nanochannels by the application of an external electric field were primarily motivated by the desire to detect the sequences of bases in a DNA or a RNA molecule. Depending on the number and sequence of bases, there is variation in the translocation speed of an electric field driven polymer in a nanoconfinement. Accordingly, by measuring the translocation characteristics of a polymer, one can infer about the sequences of bases in the molecule. One of the earliest studies in this regard dates back to the contribution of Kasianowicz et al. [143], who applied an electric field to transport single-stranded RNA and DNA molecules through a 2.6-nm diameter ion channel in a lipid bilayer membrane. Their proposed method was described as an important step towards utilizing nanoscale polymer transport for high speed detection of sequence of bases in single DNA and RNA molecules. Their study was advanced further by Meller et al. [144], who used electric field to drive DNA molecules of different lengths through  $\alpha$ -hemolysin channel in a lipid bilayer. They showed that by measuring the time for translocation as well as the current established during the translocation, one can differentiate between DNA molecules having identical length and composition but differing by sequences. They also established the possible effects of temperature variation on the translocation times. In another study [145], this group was able to precisely measure the electric field induced polymer translocation velocity and demonstrated that the polymers longer than the pore are translocated at a constant speed, but the velocity of shorter polymers increases with decreasing length. Henrickson et al. [146] used electrically-driven DNA molecules in an  $\alpha$ -hemolysin channel to obtain the scaling dependence of the blockade frequency on the applied voltage. Vocks et al. [147] quantified the corresponding blockade time (inverse of the blockade frequency) as a function of the polymer length  $N$  and the applied electric field strength. Slonkina and Kolomeiski [148] established that the size and the geometry of the nanopore are most critical in dictating the polymer translocation times. All the above mentioned studies utilized the natural protein nanopores that are mostly neutral. Very recently, researchers have tried to genetically engineer the  $\alpha$ -hemolysin nanopores (by modulating their surfaces with charges typically opposite to that of the polymer) to obtain faster translocation characteristics [149,150]. Similarly there are also examples of measuring polymer translocation characteristics in synthetic nanopores [151-153]. Most of these predictions are primarily based on the theoretical result for voltage driven polymer translocation through a nanopore which states that the translocation time  $\tau \sim NV$ , where  $N$  is the polymer size and  $V$  is the externally applied voltage. Murphy and Muthukumar [154] studied large number of polymers varying over two orders of magnitude in the molecular weight to provide concrete evidence of this scaling behaviour. This scaling relationship is based on the assumption that the translocation process is slow enough so as to ensure that the chain attains equilibrium during translocation [155-158]. In case the translocation is fast, a different scaling result of the form  $\tau \sim N^{1+\nu}/V$  (where  $\nu$  is the Flory's exponent) is used [159]. Gauthier and Slater [68] provided a different view on the possible situations in case such equilibrium assumption does not hold true. However there are contradictions to the above results as established by Storm et al. [160], who demonstrated that the translocation time scales as  $\tau \sim N^{2\nu}$ . Causes of such conflicting results were finally explained by Luo et al. [50]. Through a microscopic description of the polymer-pore interaction, they established that the polymer translocation time can be divided into three regimes: time for filling the pore, time for transfer of the polymer molecule from the *cis* (high concentration) to the *trans* (low concentration) side, and finally the time for emptying the pore. The time for emptying the pore involves an activation barrier and may completely dominate the other two time spans, particularly in presence of strong polymer-pore attractive influences. Under these conditions, the total translocation time may be described to have a dependence on the polymer of length  $N$  through effective scaling exponents that

are functions of the strength of the attractive interactions and the employed voltages [68,154,159,160]. In an earlier study, Tian and Smith [44] had shown that in presence of such attractive polymer-wall interactions, the translocation process is hastened up. However, this result directly contradicted the existing experimental findings of Meller et al. [144,162]. Luo et al. [51] also provided an explanation to this discrepancy. They used Langevin dynamics to establish that with an increase in the polymer-pore attraction, the histogram for the translocation time distribution changed from a Gaussian to a long tailed distribution corresponding to thermal activation over a free energy barrier. The size dependence of the confinement induced entropic force ensures that the polymer translocation and the residence time in the pore is a nonmonotonic function of the polymer length for short chains in the strong attraction limit. This conclusion helped to explain the differences in the results of the existing literature [44,144,162] and were also in tune with the other experimental findings [163,164]. Iqbal et al. [165] proposed a new method to use electric field driven DNA transport in nanochannels for DNA sequencing. They fabricated solid state nanopore channels that are selective towards single stranded DNA (ss-DNA). These nanopores were functionalized with a 'probe' of hair-pin loop DNA, thereby allowing selective transport of short lengths of 'target' ssDNA that are complementary to the probe. Even a single base mismatch between the probe and the target results in longer translocation pulses, thereby helping to establish the sequences of the targets. Other noteworthy investigations on sequence identification of DNA molecules using nanoscale electrophoretic DNA transport included those by Yan and Xu [166], Lagerqvist et al. [167], Zhao et al. [168], Liang and Chou [169], Clarke et al. [170] etc.

Other than the measurement of sequence of bases in the transported DNA and RNA molecules and characterizing the nanoconfined polymer translocation, electric field has also been used to drive the polymers through nanoconfinements in an effort to unravel its different other characteristics. In a pioneering study, Bakajin et al. [171] used electric field to drive DNA molecules in a thin specially designed nanoslit where they were made to interact with obstacles to elucidate the effects of confinements on the polymer dynamics. They established that notionally the effect of electric field on a polymer molecule is equivalent to the effect of a hydrodynamic flow. In a similar study executed very recently, Laachi et al. [172] used electric field for nanopore DNA translocation and in the process studied the unhooking of a long DNA chain from an isolated stationary micropost. Their investigation was useful for quickly and efficiently providing full probability distribution of the unhooking time and the ensuing moments for a wide range of chain and field parameters. Turner et al. [173] employed electric field to drive DNA molecules in a nanofluidic device partway across the interface of two regions that produce different configuration entropies. When the field was switched off, it was found that the molecules would recoil to higher entropy regions and have the profile characteristic of a force localized to the interface and independent of the length. In a similar approach, Reccius et al. [12] electrophoretically compressed the DNA molecules to drive them into nanopores. By switching off the electric field, they observed the ensuing confinement induced relaxation dynamics of the DNA molecules, which was explained by a variant of the de Gennes model. Forrey and Muthukumar [174] investigated electric field driven translocation of DNA molecules in nanopores to demonstrate the formation ds-DNA hairpins, and established that the translocation time is a function of the hairpin vertex location along the polymer backbone. They also reported the voltage dependence of the tendency of the hairpins to serve as initiators of translocation events. Mohan et al. [175] established a stochastic model to study the effect of inhomogeneous charge distribution on the polymer molecule on the translocation characteristics through a nanopore. Matysiak et al. [66] used MDS to validate the experimental findings of polymer translocation through nanopores. Their study included the aspects of the identification of two translocation regimes depending on the ratio of the pore and polymer length, identification of two different voltage dependent regimes for the probability of the translocation, characterization of the translocation velocity based on the applied voltage, and characterization of the translocation time and temperature relationship. Electric field driven transport of DNA molecules in microfabricated nanofluidic chambers has also been very widely used to separate long DNA molecules [176-180]. Other notable examples of characterizing polymer properties and behaviour by driving them electrically through nanoconfinements include the investigations on use of solid state nanopores as

microscopes for observing individual DNA molecules and their folding [151], attaining reductions in the speed of DNA translocation in solid state nanopore for efficient single molecule detection [181], achieving restriction mapping of DNA molecules using restriction endonucleases in nanochannels [182], precisely determining DNA length, diameter and conformation [183], simulating detection of proteins by genetically engineered  $\alpha$ -hemolysin channel [184], pinpointing the effect of inhomogeneity in polymer structure on translocation time [185], identifying the effect of temperature on the translocation time in the nanopore [186], studying electromechanical properties of DNA molecules by forcing single hairpin DNA molecules to translocate through nanopores [187], characterizing the dependence of unzipping kinetics of long DNA duplexes in  $\alpha$ -hemolysin pores on the shape of the base-pairing energy landscape [188, 189], studying the dependence of escape dynamics of DNA hairpins (threaded into an  $\alpha$ -hemolysin channel) on its orientations [190], discriminating (based on orientation) single-stranded DNA inside  $\alpha$ -hemolysin channel [191], investigating conformational analysis of single DNA molecules subjected to combined electrophoretic and entropic motion in nanochannels [192], achieving sequence-specific detection of individual DNA polymerase complexes using a nanopore [193], precisely measuring DNA conformation, length and speed by electrohydrodynamically stretching DNA molecules in nanochannels [194] etc.

## 5.2 Transport of nanoconfined polymer in presence of mechanical forces

The obvious advantages involved with driving flexible charged polymers through nanoconfinements by application of external electric fields are associated with inherent technological difficulties in assembling electrodes within nanoconfinements and the possible temperature rises due to Joule heating. Hence, in many cases, researchers have applied simple mechanical forces on a particular end of a polymer for transporting it through the confinements. Typically, studies on nanoconfined polymer transport in presence of an external mechanical force can be classified into two categories: a) those in which the external force causes unzipping of the DNA strands in the nanopore and results in a subsequent translocation, and b) those where the external force is used to measure other characteristics of a nanoconfined polymer.

There have a large number of investigations exploring the unzipping kinetics of DNA and RNA molecules in presence of an external force in unconfined systems. Sauer-Budge et al. [195] were among the earlier researchers to investigate force-induced unzipping kinetics of a DNA molecule in a nanopore. They calculated the unzipping time for each molecule from the ionic current signature of DNA traversal. They used a simple kinetic model to fit the distribution of unzipping times under various experimental conditions and estimated the enthalpy barriers to unzipping and the effective charge of a nucleotide in the pore. On similar lines, Mathe et al. [196] employed a nanometer scale  $\alpha$ -hemolysin pore to establish the unzipping kinetics of individual DNA hairpins in presence of constant external forces. They also studied [197] unzipping kinetics of individual DNA molecules using nanopore force spectroscopy under varying conditions of temperature and voltage ramp rates. They demonstrated that depending on the ramp rates of the applied voltages there are two unzipping regimes: for low ramp rates the unzipping obeys quasi-equilibrium characteristics but for larger ramp rates unzipping becomes irreversible. Dudko et al. [198, 199] used similar force spectroscopy method for extracting kinetic information on the nanopore DNA unzipping.

For the cases in which the force induced polymer transport is used to provide information about the polymer transport characteristics, a very important class of study involves those where the externally applied force is used to resist translocation due to other effects. For example, Kafri et al. [200] applied an external field to oppose the nanopore translocation of RNA or DNA molecules under the bias of different chemical environments on the two sides of the membrane. Under these circumstances, they established that effect of sequence heterogeneity on the polymer translocation across the nanopore. Dekker and his coworkers [201,202] demonstrated the effect of an external force in resisting the voltage-driven translocation of a DNA molecule in a nanopore. This arrests the voltage-driven DNA translocation and allows precise measurement of force on a DNA molecule in a nanopore.

Perhaps the most important study involving forced translocation of nanoconfined polymer is obtaining the scaling of translocation time with the applied force. Kantor and Kardar [159] were among the first group of researchers to quantify the translocation time as a function of the polymer length  $N$  for the case where there is an applied force. Their analysis demonstrated that under the conditions in which the translocation of a polymer through a nanopore occurs in a manner such that its two segments at the two sides of the pore are in equilibrium, the translocation dynamics is typically diffusing in nature. Thus, for such cases the translocation time varies as  $N^2$  in absence of any applied force, and as  $N$  in presence of an external force. However, for cases in which such equilibrium assumption breaks down for sufficiently long polymers, the translocation time in presence of the applied force increases and scales as  $N^{1+\nu}$ . Luo et al. [203,204] used MC simulation and Langevin dynamics study to show that for the force translocation, the scaling exponents take values of 1.5 and 1.65 for relatively short and longer chains, respectively. Dubbeldam et al. [205] proceeded one step further to demonstrate that the translocated number of monomer segments ( $s(t)$ ) displays an anomalous diffusive behaviour even in presence of an external force. Surprisingly, this anomalous dynamics of the translocation process depends on the same universal constant  $\alpha'$  ( $\alpha' = 2/(2 + 2\nu - \gamma_1)$ ; where  $\gamma_1$  is the surface exponent), exhibiting

the following scaling dependences:  $\tau \propto f^{-1} N^{\frac{2}{\alpha'-1}}$  (where  $f$  is the externally applied force),  $\langle s(t) \rangle \propto t^{\alpha'}$  and  $\langle s(t)^2 \rangle \propto t^{2\alpha'}$ . Such force dependence of the translocation time was further elaborated in the works

of Huopaniemi et al. [48]. They showed that in presence of the pulling force  $f$ , the translocation time for narrow enough pores varies as inverse of the strength of the force, for moderate strength of the force. Panja and Barkema [206] demonstrated the three dimensional nature of the polymer translocation through a nanopore in presence of an external force ( $f$ ) and established that for low to moderate forces

$\frac{fN^{\nu}}{k_B T} \leq 1$  and  $\tau \sim N^2$  (independent of  $f$ ), whereas for large enough forces  $\frac{fN^{\nu}}{k_B T} \gg 1$  and  $\tau \sim N^2/f$ . Luo et al.

[82] finally summarized the different scaling exponents for a force-driven polymer translocation through a nanopore for both two dimensional and three dimensional cases.

Among other studies of force-driven translocation of nanoconfined polymer, some of the worth mentioning ones include investigation of force-driven translocation of homopolymers through a nanopore (by MC simulation) establishing that on either sides of a critical value of temperature the translocation time shows opposite trend with temperature [207], study of nanopore translocation of heteropolymer and the effect of variation in the monomer sequences on the translocation dynamics [208], Langevin dynamics study of polymer-pore interaction on the translocation [209,210], investigation of effect of sequences on the DNA translocation through a nanopore [51] etc.

### 5.3 Transport of nanoconfined polymer in presence of other external influences

Other than the electrical and mechanical forces, factors like difference in chemical potential, thermal motion, variable adsorptive behaviour etc. have been utilized to drive polymer molecules in nanoconfinements. In one of the early works, Sung and Park [211] constructed a statistical model of polymer translocation through a nanopore driven under the influences of transmembrane chemical potential differences and Brownian ratchets. Muthukumar [212] calculated the average residence time ( $\tau$ ) of a polymer of length  $N$  passing through a nanopore under the influence of a chemical potential gradient ( $\Delta\mu$ ). He established that in absence of  $\Delta\mu$ ,  $\tau \sim N^2$  (i.e., the result of no force translocation is reproduced), whereas in presence of  $\Delta\mu$ ,  $\tau \propto \frac{NT}{k_0 \Delta\mu}$ , (for large  $\frac{N\Delta\mu}{T}$  and translocation in the direction of the chemical potential gradient; where  $T$  is the absolute temperature and  $k_0$  is rate constant of polymer translocation across the pore),  $\tau \propto \frac{N^2}{k_0}$  (for small  $\frac{N\Delta\mu}{T}$  and translocation in the direction of the chemical potential gradient), and  $\tau \sim \exp(N)$  (for translocation against the direction of the chemical potential

gradient). Muthukumar [158] also investigated the translocation dynamics (by measuring the free energy barrier and mean translocation time) of the passage of a single Gaussian chain from one sphere to another larger sphere through a nanopore in presence of a chemical potential gradient. Tian and Smith [44] employed BDS to investigate chemical potential gradient driven translocation of single polymer chains through nanopores. Chan et al. [213] established the role of competitive influences of free energy barrier ( $F_b$ ) and chemical potential gradient ( $\Delta\mu$ ) on the nanopore translocation dynamics of polymer chains. They established that the relaxation time was dictated by  $F_b$ , whereas the escaping time is primarily dominated by  $\Delta\mu$ . Xie et al. [214] established the influences of volume exclusion effects in the translocation of polymer chain from a source container to a drain container through a short nanochannel, driven by the large chemical potential difference between polymer segments in the source container and those in the drain container. Luo [215] used MC simulations to study the translocation of polymer chains through an interacting nanopore from a confined environment (*cis* side, high concentration of chain) to a spacious environment (*trans* side, zero concentration). They demonstrated that attractive polymer-pore interaction hastens the translocation, and the optimal value of this interaction for which the polymer acceleration is the fastest increases with an increment in the concentration of the chain on the *cis* side.

Polymer translocation can also occur by differential adsorption of a polymer across the pore. For example, Park and Sung [216] demonstrated polymer translocation through a nanopore in a membrane caused by its adsorption in the *trans* side of the membrane. They established that when the system temperature ( $T$ ) was more than the adsorption-desorption transition temperature ( $T_c$ ), translocation time ( $\tau$ ) scales as  $\tau \sim L_c^3$  (where  $L_c$  is the polymer contour length) and for  $T < T_c$ ,  $\tau \sim L_c^2$ . On similar lines, Milchev et al. [217] obtained the translocation dynamics of a flexible macromolecule through a nanopore under the assumption that the driving force was provided by purely repulsive polymer-wall interaction in the *cis* side and attractive polymer-wall interaction in the *trans* side.

Other than studying these polymer translocations by employing these different forcing mechanisms, there have also been significant numbers of studies that delineate transport of nanoconfined polymer molecules in the absence of external forces. Some such notable contributions include the works by Wolterink et al. [218], Panja et al. [219,220], Dubbeldam et al. [221], Luo and his coworkers [204,222], Wei et al. [49], Guillouzie et al. [223] etc.

#### 5.4 Transport of nanoconfined polymer in presence of flow field

Technological challenges associated with establishing controllable fluid flows in nanoscale confinements have been primarily responsible in the slow progresses towards understanding the details of transport phenomena in nanoconfined polymers in presence of flow fields. However, over the last few years, the researchers have been successful in achieving several important technological breakthroughs associated with the flow driven polymer in nanochannels. One of the most important revelations has been the understanding of how the flow field affects the polymer chain density distribution across the channel (see Section 4.1). It has been revealed that the flow field makes the chain density steeper (i.e., more displaced from the wall), quantifying to an increase in the depletion layer thickness.

As has been already established (see section 5.1), electric field induced transport has been a widely practiced method of driving a nanoconfined polymer. However, in most of the concerned studies, the influences of electroosmotic flow [33] have been ignored. A pioneering study on electroosmotic flow driven transport of nanoconfined polymer was by Bakajin et al. [171]. In presence of the applied field, these authors assumed that the DNA molecules are being subjected to a uniform flow field and obtained the polymer stretching as a function of the flow velocity. Gasparac et al. [224] employed a transmembrane electric field to drive DNA molecules through a nanopore by a combined electrophoretic and electroosmotic transport. Ghosal [225] established the effect of hydrodynamics in the electrophoretic nanopore translocation of a polymer molecule. He described the polymer motion in terms of the established electroosmotic flow field for vanishingly small Debye length and the resulting pressure-induced flow. In another work [226], he introduced the effect of finite Debye layer (i.e., the effect of salt concentration) on the resulting electroosmotic transport in the course of electrophoretic motion of the

polymer in a nanopore. He also introduced the effect of a uniform surface charge on the walls of the nanopore and the calculated transit times were found to show good match with experiments. He established the possible consequence of electroosmotic flow induced viscous drag on a tethered DNA molecule inside a nanopore [227]. It was seen that the reductions in the tether force due to viscous drag and due to charge reduction by Manning condensation were of similar size. Wong and Muthukumar [228] considered electroosmotic flow induced polymer transport in nanopores having charge of opposite sign as the polymers. They established that due to the generation of large electric field across the nanopore in DNA translocation experiments, electroosmotic flow creates a large absorbing region of size comparable to the polymer around the nanopore. Pennathur et al. [229] employed electroosmotic transport for free solution oligonucleotide separation in nanoscale channels. Liang et al. [230] used combined electrophoretic and electroosmotic transport to drive and stretch DNA molecules in nanofluidic channels fabricated by novel nanoimprint mold fabrication and direct imprinting. Magila et al. [149] established that by using a combined electroosmotic and electrophoretic transport, they can modulate the internal positive charge of a  $\alpha$ -hemolysin nanopore to hasten up the translocation of a single DNA molecule. Luan and Aleksei [231] performed an all atom MDS to establish that in a nanopore in presence of an external electric field ( $E$ ), the induced electroosmotic transport around the DNA surface (induced by the motion of the counterions in the vicinity of the DNA molecule) created a hydrodynamic drag that caused a reduction in the effective DNA charge. Consequently the net electric force ( $F_{el}$ ) on the DNA molecule read  $F_{el} = \xi \mu_{ep} E$  (where  $\xi$  and  $\mu_{ep}$  are the friction coefficient and electrophoretic mobility of DNA, respectively). In a very recent fundamental study, van Dorp et al. [232] performed extensive experiments to pinpoint the possible role of hydrodynamics and ionic screening on the origin of electrophoretic force on DNA in solid-state nanopores.

Other than the electroosmotic transport, pressure-driven transport is also commonly used to study flow induced polymer dynamics in nanoconfinements. For example, many researchers have employed Poiseuille flow to study the polymer chain distribution across the nanochannels and have pinpointed the differences in comparison to the case without the flow field [31, 43, 83, 84, 111]. In a similar example, Webster and Yeomans [233] used a multiscale algorithm to study the dynamics of a tethered polymer in a nanoslit in presence of Poiseuille flow. Stein et al. [234] employed fluorescence microscopy to investigate pressure-driven transport of individual DNA molecules in silica nanochannels and microchannels. They identified two distinct transport regimes depending on the channel height. For channels of height few times the DNA radius of gyration, pressure-driven DNA mobility increased with molecular length, but for thin nanochannels the DNA mobility was virtually independent of molecular length. Khare et al. [43] used MDS to demonstrate that such Poiseuille flow can cause very large temperature rises in the bulk. This, in turn, may cause a preferential polymer transport away from the bulk and lead to chain density distribution with two off-center peaks (the strength of the peaks increases with an increase in the pressure-driven velocity, as also established by our BDS study [31]; see Fig. 7). In fact, we [31] went one step ahead to show that possible considerations of streaming potential influences imply that the strength of such off-center peaks turn out to be strong functions of the parameters that control the streaming potential, namely the wall charge density and the bulk ionic concentration (see Fig. 8). We also showed that with the aid of an opposing external electroosmotic flow, in conjunction with this pressure-driven flow and streaming field induced back electrokinetic transport, the shear rate in the flow field can be judiciously manipulated to obtain polymer chain distribution with very steep off-center peaks, signifying strengthening of the effective confinement of the polymers (see Fig. 9). Zhang et al. [235] used all atom non-equilibrium MDS to elucidate structural and dynamical properties of highly confined linear polymer fluids undergoing planar Poiseuille flows. Schoch et al. [236] demonstrated that diffusion-limited binding of the macromolecules can be distinctly augmented in case the molecules are steered into nanochannels by either electrokinetic or pressure-driven transport. For large flow speeds, the ensued reaction kinetics enhancement is dictated by the force-induced dissociation of receptor-ligand bonds. Consequently, when optimized, this scheme can be successfully used for label-free electrical detection of biomolecules. Abgrall and Nguyen [237] reviewed the benefits in nanofluidic separation of polymers in presence of shear-driven and pressure-driven transport.

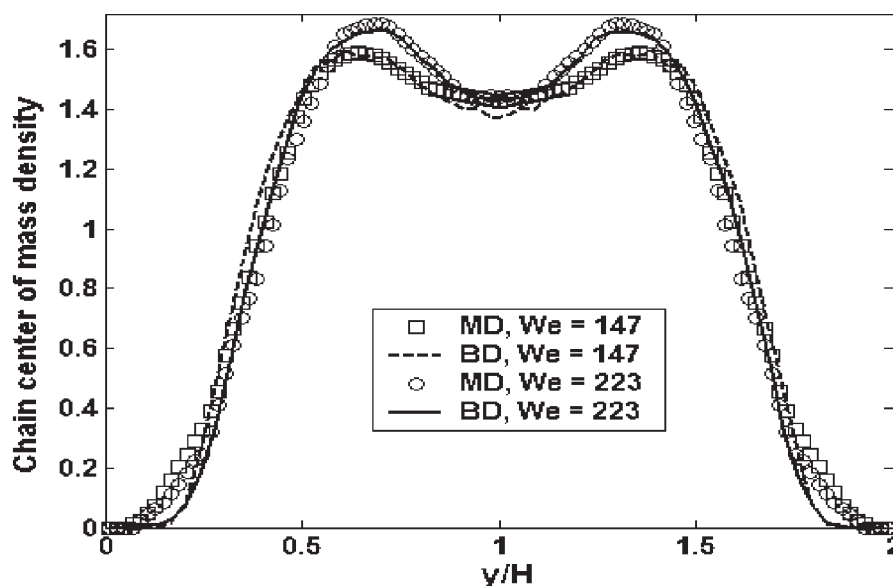


Figure 7. Chain center of mass distribution for a 20-bead chain for the equilibrium case and the case with an externally imposed Poiseuille flow field (strength of the characterized by the different values of Weissenberg number ( $We$ ), calculated based on the effective shear rate of the of the Poiseuille flow  $\dot{\gamma} = V_{max} / (h / 2)$ , where  $V_{max}$  is the maximum of the Poiseuille velocity and  $h$  is the channel height). The figure illustrates the effect of temperature rise due to the existing shear rate gradient in causing a chain center of mass distribution with two off center peaks.

In this figure  $z$  represents the dimensionless transverse distance (made dimensionless with LJ unit distance  $\sigma_{LJ,w} = 0.31656 \text{ nm}$ ). (Other parameters that are used  $\rho$  (density) = 0.6,  $T_{wall} = 1.5$ , and chain mass fraction = 0.0116. All these values are referenced on the following LJ scales for typical water molecules:  $\sigma_{LJ,w} = 0.31656 \text{ nm}$ ,  $m = 2.99 \times 10^{-26} \text{ kg}$  and  $\epsilon_{LJ,w} = 0.65 \text{ kJ/mol}$ .)

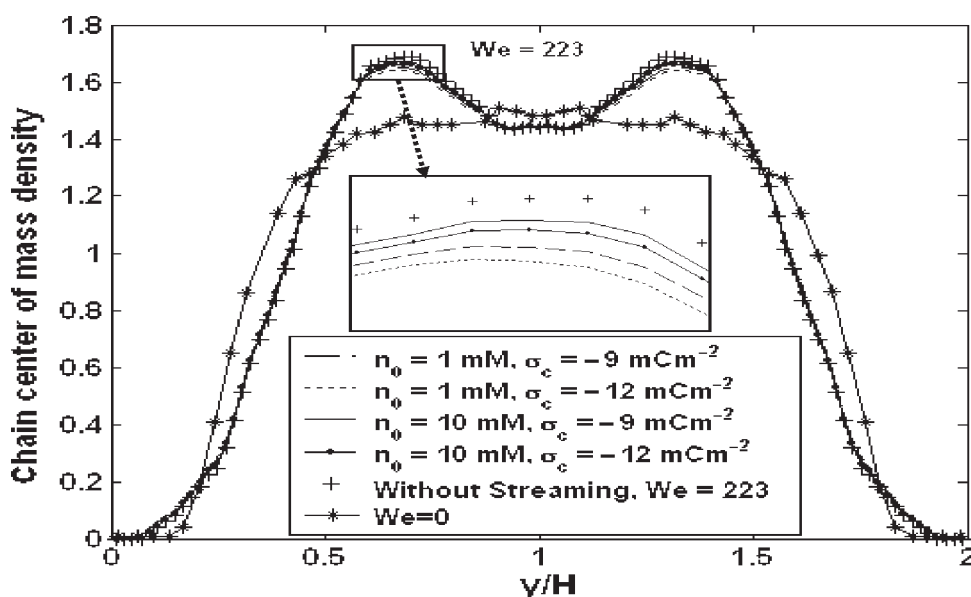


Figure 8. Chain center of mass density profiles across the channel section for a 20-bead chain for different values of bulk ionic concentration and surface charge density (Higher values of charge density and lower values of bulk ionic concentration yield larger streaming current). This plot considers pure pressure-driven transport and the consequences of the streaming current are included. Results are compared to the cases with no streaming effect considerations.  $We$  is considered to be 223 for all cases. In the *inset* we demonstrate the magnified portion near the left peak.

It is seen that the effect of streaming field induced lowering of the velocity field lowers the shear rate causing a lowering in the strength of the off center peaks.

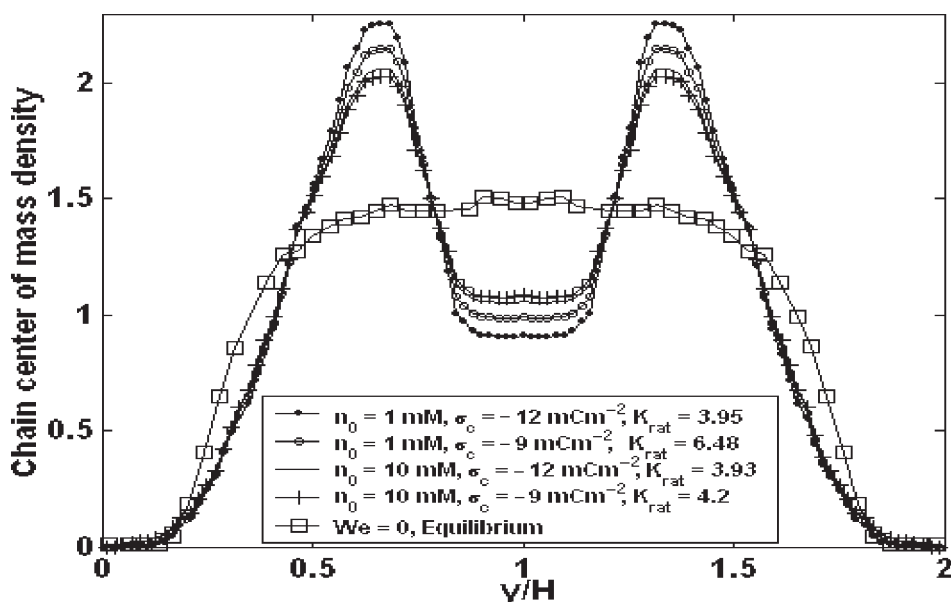


Figure 9. Chain center of mass density profiles across the channel section for a 20-bead chain for different values of bulk ionic concentration and surface charge density (Higher values of charge density and lower values of bulk ionic concentration yield larger streaming current). This plot considers combined pressure-driven and electroosmotic transport (the external electroosmotic transport is so initiated that it opposes the pressure-driven transport) and the consequences of the streaming current are included. Corresponding to a given combination of the bulk ionic concentration and surface charge density, the optimized value of  $K_{rat}$  ( $K_{rat} = u_{HS} / u_{p,max}$ ,  $K_{rat} = u_{HS} / u_{p,max}$ , i.e., ratio of the maximum electroosmotic velocity and the pressure-driven velocity) is identified and the chain center of mass density profiles are obtained at that value of  $K_{rat}$  (as indicated in the plot).

The plot shows that consideration of streaming influences for a judiciously driven flow field (i.e., a well-designed combination of electroosmotic and pressure-driven flow) greatly increases the strengths of the off-center peaks indicating a much larger effective confinement of the polymer chains.

There are also a number of reports that study nanoconfined polymer transport using uniform or shear-driven flow. He et al. [238] employed DPD simulations to investigate polymer translocation through a nanopore in presence of a uniform flow field of constant field strength  $E$ . He established that the translocation time ( $\tau$ ) scales with the field strength as  $\tau \sim E^{-0.48 \pm 0.01}$ . Wang and Sandberg [239, 240] employed MDS to study the properties and dynamics (stretch, rotation and relaxation) of free and end-tethered short chains of single and double stranded DNA molecules in nanochannel shear flows. Their efforts led to extremely sensitive measurements of the relaxation time (in the tune of picoseconds) and hydrodynamic force (in the tune of nano-Newtons). The velocity profiles in solution of end-tethered DNA were found to be nonlinear for large enough shear rates. Dynamics of free ss-DNA was dependent on their initial orientation with respect to the flow field. The DNA molecules were found to exhibit conformational behaviors (including coils, hairpin loops, and figure-eight shapes) that were not known before. Also, the relative proximity of the DNA molecules to the channel walls was found to be extremely critical in dictating their overall dynamics. In a very recent study, Kohale and Khare [241] employed MDS to study cross stream nanochannel migration of flexible polymers subjected to planar Couette flows. They demonstrated that longer chains are more effectively stretched by the flow field

and consequently get migrated away from the walls. On contrary, the shorter chains that are not stretched fail to exhibit such migrative tendencies.

## 6. SCOPE OF FUTURE RESEARCH

The plethora of investigations concerning transport of flexible polymer molecules in nanoconfinements has allowed tremendous advances in our knowledge about the structure of polymer molecules, and has helped to perform a large number of important bioanalytical activities like DNA sequencing, separation of long length DNA molecules, characterizing the conformational behaviour of DNA etc. Important research breakthroughs on these issues have been discussed in details in the previous sections. Advances on different issues of nanofabrication allow continuous improvements in handling single polymer molecules in nanochannels, thereby permitting continuous developments of devices and applications involving nanoconfined polymers. However, there are still a number of issues concerning transport of nanoconfined polymers that are beyond the understanding and the expertise of the research communities. Future research endeavours need to be directed in a manner so as to address these yet unresolved issues.

One of the major bottlenecks of handling polymers in nanoconfinements is the disadvantage associated with handling large polymers. In fact, in most of the successful experiments involving nanoconfined polymers, the polymers are typically very short. Larger polymers invariably encounter larger entropic barriers during their transport from the bulk into the confinement, thereby requiring a larger pulling influence. However, it needs to be ensured that such pulling force is not exerted in a manner that will disrupt the polymer configuration (such disruption can be in form of local unzipping and may dynamically alter the polymer characteristics). Such controlled application of large force-induced polymer transport in nanofluidic confinements remains a topic of great exploration in the near future.

Unwanted surface adsorption of polymers and the resulting blockage of nanochannels during transport of nanoconfined polymers have long haunted the researchers [242–244]. The concerning issues stem from the fact that within the nanochannel, the polymer dynamics is primarily dictated by the extent of confinement, enforcing a very limited external controllability. Consequently, a judicious selection of the nanochannel substrate, based on the choice of the polymer to be transported, becomes imperative. Most of the modern day nanofluidic applications being based on artificially prepared nanochannels, there is huge scope of research, particularly for material scientists, to design intelligent materials that will behave desirously with a wide range of polymers and at the same time should be alterable at the nanometer scale.

The role of polymer transport in nanofluidic devices for chemical diagnostic and detection applications is yet to be well established, primarily attributed to device expenses as well as poor controllability of the target analytes. Thus, the advantages associated with confinement induced chemical detection processes are yet to be practically realized down to nanometer length scales. However, with rapidly increasing requirements for detection with virtually negligible target analyte concentrations, efforts need to be directed to design efficient nanofluidic chips that can detect target DNA composition by hybridizing with its complementary strand immobilized at the nanochannel surface. Such techniques, though well known over micrometer scales, need to be further downscaled to achieve these feats.

## 7. CONCLUSIONS

In this article, a brief review of recent advancements in the science and technology of polymer transport in nanofluidic confinements has been presented. It has been inferred that the interplay between the system length scales (dictated by the extent of confinements) and the length scales pertaining to the conformational freedom of the polymer gives rise to intriguing polymer dynamical responses. We have discussed the possible nature and quantification of such responses in a somewhat abridged manner. We have also highlighted possible intriguing interactions between the polymer

molecule and the nanochannel wall over nanometer and sub-nanometer length scales. The non-trivialities associated with such interactions enforce a kind of polymer response that can be accounted for only through relevant quasi-continuum, mesoscopic, and non-continuum approaches. Such approaches, their merits and demerits, as well as their respective applicabilities according to the context have also been elaborately discussed. Other consequences of strong confinements like the formation of depletion layer, sinusoidal mass density distribution etc. have also been delineated. Further, the competing influences of the external driving forces, in relation to the entropic effects induced by the confinements towards altering the polymer dynamics in nanochannels have been pinpointed. Finally, the possible directions in which the future research on nanoconfined polymer systems needs to proceed have been discussed.

## REFERENCES

- [1] P.G. de Gennes, *Scaling Concepts in Polymer Physics*, 1979, Cornell University Press, Ithaca, NY.
- [2] T. Odijk, On the statistics and dynamics of confined or entangled stiff polymers, *Macromolecules*, 1983, 16, 1340-1344.
- [3] L. Yang, I. Akhatov, M. Mahinfalah, and B.Z. Jang, Nano-fabrication: A review, *J. Chin. Inst. Eng.*, 2007, 30, 441-446.
- [4] B.D. Gates, Q. Xu, M. Stewart, D. Ryan, C.G. Willson, and G.M. Whitesides, New approaches to nanofabrication: Molding, printing, and other techniques, *Chem. Rev.*, 2005, 105, 1171-1196.
- [5] K. Ariga and H.S. Nalwa, *Bottom-up Nanofabrication: Supramolecules, Self-Assemblies and Organized Films*, 2006, American Scientific Publishers.
- [6] I. Teraoka, *Polymer Solutions: An Introduction to Physical Properties*, 2002, Wiley-Interscience.
- [7] S.F. Sun, *Physical Chemistry of Macromolecules: Basic Principles and Issues*, 2004, Wiley-Interscience.
- [8] D.C. Morse, Viscoelasticity of Concentrated Isotropic Solutions of Semiflexible Polymers. 2. Linear Response, *Macromolecules*, 1998, 31, 7044-7067.
- [9] G.K. Batchelor, *An Introduction to Fluid Dynamics*, 1967, Cambridge University Press, Cambridge, England.
- [10] J.O. Tegenfeldt, C. Prinz, H. Cao, S. Chou, W.W. Reisner, R. Riehn, Y.M. Wang, E.C. Cox, J.C. Sturm, P. Silberzan, and R.H. Austin, The dynamics of genomic-length DNA molecules in 100-nm channels, *Proc. Nat. Acad. Sci. USA*, 2004, 101, 10979-10983.
- [11] W. Reisner, K.J. Morton, R. Riehn, Y.M. Wang, Z. Yu, M. Rosen, J.C. Sturm, S.Y. Chou, E. Frey, and R.H. Austin, Statics and dynamics of single DNA molecules confined in nanochannels, *Phys. Rev. Lett.* 2005, 94, 196101 (1-4).
- [12] C.H. Reccius, J.T. Mannion, J.D. Cross, and H.G. Craighead, Compression and free expansion of single DNA Molecules in nanochannels. *Phys. Rev. Lett.*, 2005, 95, 268101 (1-4).
- [13] P.-K. Lin, C.-C. Fu, Y.-L. Chen, Y.-R. Chen, P.-K. Wei, C.H. Kuan, and W.S. Fann, Static conformation and dynamics of single DNA molecules confined in nanoslits, *Phys. Rev. E*, 2007, 76, 011806 (1-8).
- [14] J.D. Cross, E.A. Strychalski, and H.G. Craighead, Size-dependent DNA mobility in nanochannels, *J. App. Phys.*, 2007, 102, 024701 (1-5).
- [15] A. Balducci, P. Mao, J. Han, and P.S. Doyle, Double-stranded DNA diffusion in slitlike nanochannels, *Macromolecules*, 2006, 39, 6273-6281.
- [16] D.J. Bonthuis, C. Meyer, D. Stein, and C. Dekker, Conformation and dynamics of DNA Confined in slitlike nanofluidic channels, *Phys. Rev. Lett.* 2008, 101, 108303 (1-4).
- [17] T. Odijk, Scaling theory of DNA confined in nanochannels and nanoslits, *Phys. Rev. E*, 2008, 77, 060901 (1-4).

- [18] L.H. Thamdrup, A. Klukowska, and A. Kristensen, Stretching DNA in polymer nanochannels fabricated by thermal imprint in PMMA, *Nanotechnology*, 2008, 19, 125301 (1-6).
- [19] K.D. Park, S.W. Lee, N. Takama, T. Fujii, and B.J. Kim, Arbitrary-shaped nanochannels fabricated by polymeric deformation to achieve single DNA stretching, *Microelec. Eng.*, 2009, 86, 1385-1388.
- [20] Y. Chen and M. Muthukumar, Free energy of a molecule in a confined domain, *Phys. Rev. B*, 1986, 33, 6187-6190.
- [21] F. Wagner, G. Lattanzi, and E. Frey, Conformations of confined biopolymers, *Phys. Rev. E*, 2007, 75, 050902(R) (1-4).
- [22] Y. Yang, T.W. Burkhardt, and G. Gompper, Free energy and extension of a semiflexible polymer in cylindrical confining geometries, *Phys. Rev. E*, 2007, 76, 011804 (1-7).
- [23] A. Arnold, B. Bozorgui, D. Frenkel, B.-Y. Ha, and S. Jun, Unexpected relaxation dynamics of a self-avoiding polymer in cylindrical confinement, *J. Chem. Phys.*, 2007, 127, 164903 (1-9).
- [24] T. Sakaue, Semiflexible polymer confined in closed spaces, *Macromolecules*, 2007, 40, 5206-5211.
- [25] L.I. Klushin, A.M. Skvortsov, H.-P. Hsu, and K. Binder, Dragging a polymer chain into a nanotube and subsequent release, *Macromolecules*, 2008, 41, 5890-5898.
- [26] R.M. Jendrejack, D.C. Schwartz, M.D. Graham, and J.J. dePablo, Effect of confinement on DNA dynamics in microfluidic devices, *J. Chem. Phys.*, 2003, 119, 1165-1173.
- [27] R.M. Jendrejack, D.C. Schwartz, J.J. dePablo, and M.D. Graham, Shear induced migration in flowing polymer solutions: simulation of long chain deoxyribose nucleic acid in microchannels, *J. Chem. Phys.*, 2004, 120, 2513-2529.
- [28] R.M. Jendrejack, E.T. Dimalanta, D.C. Schwartz, M.D. Graham, and J.J. dePablo, DNA dynamics in a microchannel, *Phys. Rev. Lett.*, 2003, 91, 038102 (1-4).
- [29] R.B. Bird, C.F. Curtiss, R.C. Armstrong, and O. Hassager, *Dynamics of Polymeric Liquids*, 1987, Wiley, New York.
- [30] M. Fixman, Construction of Langevin forces in the simulation of hydrodynamic interaction, *Macromolecules*, 1986, 19, 1204-1207.
- [31] T. Das, S. Das, and S. Chakraborty, Influences of streaming potential on cross stream migration of flexible polymer molecules in nanochannel flows, *J. Chem. Phys.*, 2009, 131, 1 (1-12).
- [32] M.X. Fernandes, M.L. Huertas, M.A. R.B. Castanho, and J.G. de la Torre, Conformation and dynamic properties of a saturated hydrocarbon chain confined in a model membrane: a Brownian dynamics simulation, *Biochim. Biophys. Acta*, 2000, 1463, 131-141.
- [33] R.J. Hunter, *Zeta Potential in Colloid Science*, 1981, Academic, London.
- [34] K.S. Schmitz, *Macroions in Solutions and Colloidal Suspension*, 1993, VCH, New York.
- [35] H. Ohshima, T.W. Healy, and L.R. White, Accurate analytic expressions for the surface charge density/surface potential relationship and double-layer potential distribution for a spherical colloidal particle, *J. Coll. Int. Sci.*, 1982, 90, 17-26.
- [36] Y.C. Lin and C.P. Jen, Mechanism of hydrodynamic separation of biological objects in microchannel devices, *Lab Chip*, 2002, 2, 164-169.
- [37] S. Das and S. Chakraborty, Electrokinetic separation of charged macromolecules in nanochannels within the continuum regime: Effects of wall interactions and hydrodynamic confinements, *Electrophoresis*, 2008, 29, 1115-1124.
- [38] S. Das and S. Chakraborty, Transport and Separation of Charged Macromolecules under Nonlinear Electromigration in Nanochannels, *Langmuir*, 2008, 24, 7704-7710.
- [39] J. Israelachvili, *Intermolecular and Surface Forces. 2 ed.*, 2003, Academic Press, London.
- [40] A. Majumdar and I. Mezic, Stability regimes of thin liquid films, *Microsc. Thermophys. Eng.*, 1998, 2, 203-213.

- [41] S. Chakraborty and S. Das, Streaming-field-induced convective transport and its influence on the electroviscous effects in narrow fluidic confinement beyond the Debye-Hückel limit, *Phys. Rev. E*, 2008, 77, 037303 (1-4).
- [42] J.K.G. Dhont, Thermodiffusion of interacting colloids, *J. Chem. Phys.*, 2004, 120, 1642-1653.
- [43] R. Khare, M.D. Graham, and de Pablo, Cross-stream migration of flexible molecules in a nanochannel, *Phys. Rev. Lett.*, 2006, 96, 226405 (1-4).
- [44] P. Tian and G.D. Smith, Translocation of a polymer chain across a nanopore: A Brownian dynamics simulation study, *J. Chem. Phys.*, 2003, 119, 11475-11483.
- [45] J. Wang and H. Gao, A generalized bead-rod model for Brownian dynamics simulations of wormlike chains under strong confinement, *J. Chem. Phys.*, 2005, 123, 084906 (1-13).
- [46] J.P. Hernández-Ortiz, J.J. de Pablo, and M.D. Graham, Fast computation of many-particle hydrodynamic and electrostatic interactions in a confined geometry, *Phys. Rev. Lett.*, 2007, 98, 140602 (1-4).
- [47] Y.-L. Chen, H. Ma, M.D. Graham, and J.J. de Pablo, Modeling DNA in confinement: A comparison between the Brownian Dynamics and Lattice Boltzmann method, *Macromolecules*, 2007, 40, 5978-5984.
- [48] I. Huopaniemi, K. Luo, T. Ala-Nissila, and S.-C. Ying, Polymer translocation through a nanopore under a pulling force, *Phys. Rev. E*, 2007, 75, 061912(1-6).
- [49] D. Wei, W. Yang, X. Jin, and Q. Liao, Unforced translocation of a polymer chain through a nanopore: The solvent effect, *J. Chem. Phys.*, 2007, 126, 204901 (1-8).
- [50] K. Luo, T. Ala-Nissila, S.-C. Ying, and A. Bhattacharya, Translocation dynamics with attractive nanopore-polymer interactions, *Phys. Rev. E*, 2008, 78, 061918 (1-8).
- [51] K. Luo, T. Ala-Nissila, S.-C. Ying, and A. Bhattacharya, Sequence dependence of DNA translocation through a nanopore, *Phys. Rev. Lett.*, 2008, 100, 058101 (1-4).
- [52] W. Mobius, E. Frey, and U. Gerland, Spontaneous unknotting of a polymer confined in a nanochannel, *Nano Lett.*, 2008, 8, 4518-4522.
- [53] L. Huang and D.E. Marakov, The rate constant of polymer reversal inside a pore, *J. Chem. Phys.*, 2008, 128, 114903 (1-9).
- [54] P. Prinsen, L.T. Fang, A.M. Yoffe, C.M. Knobler, and W.M. Gelbart, The force acting on a polymer partially confined in a tube, *J. Phys. Chem. B*, 2009, 113, 3872-3879.
- [55] V. Kuppa and E. Manias, Dynamics of poly (ethylene oxide) in nanoscale confinements: A computer simulations perspective, *J. Chem. Phys.*, 2003, 118, 3421-3429.
- [56] G.A. Schwartz, R. Bergman, and J. Swenson, Relaxation dynamics of a polymer in a 2D confinement, *J. Chem. Phys.*, 2004, 120, 5736-5744.
- [57] Y. Rabin and M. Tanaka, DNA in nanopores: Counterion condensation and coion depletion, *Phys. Rev. Lett.*, 2005, 94, 148103 (1-4).
- [58] A. Aksimentiev, J.B. Heng, G. Timp, and K. Schulten, Microscopic kinetics of DNA translocation through synthetic nanopores, *Biophys. J.*, 2004, 87, 2086-2097.
- [59] E.Y. Lau, F.C. Lightstone, and M.E. Colvin, Dynamics of DNA encapsulated in a hydrophobic nanotube, *Chem. Phys. Lett.*, 2005, 412, 82-87.
- [60] S.T. Cui, Molecular dynamics study of single-stranded DNA in aqueous solution confined in a nanopore, *Mol. Phys.*, 2004, 102, 139-146.
- [61] J.B. Heng, A. Aksimentiev, C. Ho, P. Marks, Y.V. Grinkova, S. Sligar, K. Schulten, and G. Timp, The electromechanics of DNA in a synthetic nanopore, *Biophys. J.*, 2006, 90, 1098-1106.
- [62] B. Luan and A. Aksimentiev, Electro-osmotic screening of the DNA charge in a nanopore, *Phys. Rev. E*, 2008, 78, 021912 (1-4).

- [63] D.I. Dimitrov, A. Milchev, K. Binder, L.I. Klushin, and A.M. Skvortsov, Universal properties of a single polymer chain in slit: Scaling versus molecular dynamics simulations, *J. Chem. Phys.*, 2008, 128, 234902 (1-11).
- [64] F. Höfling, T. Munk, E. Frey, and T. Franosch, Entangled dynamics of a stiff polymer, *Phys. Rev. E*, 2008, 77, 060904(R) (1-4).
- [65] Y. Jung, S. Jun, and B.-Y. Ha, Self-avoiding polymer trapped inside a cylindrical pore: Flory free energy and unexpected dynamics, *Phys. Rev. E*, 2009, 79, 061912 (1-8).
- [66] S. Matysiak, A. Montesi, M. Pasquali, A.B. Kolomeisky, and C. Clementi, Dynamics of polymer translocation through nanopores: Theory meets experiment, *Phys. Rev. Lett.*, 2006, 96, 118103 (1-4).
- [67] S. Melchionna, M. Bernaschi, M. Fyta, E. Kaxiras, and S. Succi, Quantized biopolymer translocation through nanopores: Departure from simple scaling, *Phys. Rev. E*, 2009, 79, 030901(R) (1-4).
- [68] M.G. Gauthier and G.W. Slater, Nondriven polymer translocation through a nanopore: Computational evidence that the escape and relaxation processes are coupled, *Phys. Rev. E*, 2009, 79, 021802 (1-7).
- [69] M. Fyta, S. Melchionna, S. Succi, and E. Kaxiras, Hydrodynamic correlations in the translocation of a biopolymer through a nanopore: Theory and multiscale simulations, *Phys. Rev. E*, 2008, 78, 036704 (1-7).
- [70] Y. Wang and I. Teraoka, Structures and thermodynamics of nondilute polymer solutions confined between parallel plates, *Macromolecules*, 2000, 33, 3478-34484.
- [71] P. Cifra and I. Teraoka, Partitioning of polymer chains in solution with a square channel: lattice Monte Carlo simulations, *Polymer*, 2002, 43, 2409-2415.
- [72] I. Teraoka, P. Cifra, and Y. Wang, Polymer chains in good solvent facing impenetrable walls: what is the distance to the wall in lattice Monte Carlo simulations, *Coll. Surf. A*, 2002, 206, 299-303.
- [73] Y. Wang, Q. Lin, P. Cifra, and I. Teraoka, Partitioning of bimodal polymer mixtures into a slit: effect of slit width, composition and pore-to-bulk volume ratio, *Coll. Surf. A*, 2002, 206, 305-312.
- [74] T. Bleha and P. Cifra, Free energy and confinement force of macromolecules in a slit at full equilibrium with a bulk solution, *Polymer*, 2003, 45, 3745-3752.
- [75] I. Teraoka and Y. Wang, Computer simulation studies on overlapping polymer chains confined in narrow channels, *Polymer*, 2004, 45, 3835-3843.
- [76] R. Bundschuh and U. Gerland, Coupled dynamics of RNA folding and nanopore translocation, *Phys. Rev. Lett.*, 2005, 95, 208104 (1-4).
- [77] A. Cacciuto and E. Luijten, Confinement-driven translocation of a flexible polymer, *Phys. Rev. Lett.*, 2006, 96, 238104 (1-4).
- [78] J. Kalb and B. Chakraborty, Single polymer confinement in a tube: Correlation between structure and dynamics, *J. Chem. Phys.*, 2009, 130, 025103 (1-9).
- [79] W. Lim, S.Y. Ng, C. Lee, Y.P. Feng, and J.R.C. van der Maarel, Conformational response of supercoiled DNA to confinement in a nanochannel, *J. Chem. Phys.*, 2008, 129, 165102 (1-6).
- [80] M.G. Gauthier and G.W. Slater, A Monte Carlo algorithm to study polymer translocation through nanopores. I. Theory and numerical approach, *J. Chem. Phys.*, 128, 065103 (1-8).
- [81] T. Cui, J. Ding, and J.Z.Y. Chen, Dynamics of a self-avoiding polymer chain in slit, tube, and cube confinements, *Phys. Rev. E*, 2008, 78, 061802 (1-7).
- [82] K. Luo, S.T.T. Ollila, I. Huopaniemi, T. Ala-Nissila, P. Pomorski, M. Karttunen, S.-C. Ying, and A. Bhattacharya, Dynamical scaling exponents for polymer translocation through a nanopore, *Phys. Rev. E*, 2008, 78, 050901(R) (1-4).

- [83] O.B. Usta, A.J.C. Ladd, and J.E. Butler, Lattice-Boltzmann simulations of the dynamics of polymer solutions in periodic and confined geometries, *J. Chem. Phys.*, 2005, 122, 094902 (1-11).
- [84] O.B. Usta, J.E. Butler and A.J.C. Ladd, Flow-induced migration of polymers in dilute solution, *Phys. Fluids*, 2006, 18, 031703 (1-4).
- [85] O.B. Usta, J.E. Butler and A.J.C. Ladd, Transverse migration of a confined polymer driven by an external force, *Phys. Rev. Lett.*, 2007, 98, 098301 (1-4).
- [86] S. Reboux, F. Capuani, N. Gonzalez-Segredo, and D. Frenkel, Lattice-Boltzmann simulations of ionic current modulation by DNA translocation, *J. Chem. Theory Comput.*, 2006, 2, 495–503.
- [87] Y. Xie, H. Yu, H. Yang, Y. Wang, X. Zhang and Q. Shi, Monte Carlo study on spontaneous recoil of confined DNA chain, *Chin. J. Chem. Phys.*, 2008, 21, 281-285.
- [88] D.A. Fedosov, G.E. Karniadakis, and B. Caswell, Dissipative particle dynamics simulation of depletion layer and polymer migration in micro- and nanochannels for dilute polymer solutions, *J. Chem. Phys.*, 2008, 128, 144903 (1-14).
- [89] J.A. Millan, W. Jiang, M. Laradji, and Y. Wang, Pressure driven flow of polymer solutions in nanoscale slit pores, *J. Chem. Phys.*, 2007, 126, 124905 (1-9).
- [90] J.A. Milan and M. Laradji, Cross-stream migration of driven polymer solutions in nanoscale channels: A numerical study with generalized dissipative particle dynamics, *Macromolecules*, 2009, 42, 803-810.
- [91] E. Moendarbary, T.Y. Ng, H. Pan, and K.Y. Lam, Migration of DNA molecules through entropic trap arrays: a dissipative particle dynamics study, *Microfluid. Nanofluid.*, DOI 10.1007/s10404-009-0463-0.
- [92] Z. Ye, J. Cai, H. Liu, and Y. Hu, Density and chain conformation profiles of square-well chains confined in a slit by density-functional theory, *J. Chem. Phys.*, 2005, 123, 194902 (1-8).
- [93] Z. Ye, H. Chen, J. Cai, H. Liu, and Y. Hu, Density functional theory of homopolymer mixtures confined in a slit, *J. Chem. Phys.*, 2006, 125, 124705 (1-7).
- [94] Z. Ye, H. Chen, H. Liu, Y. Hu, and J. Jiang, Density functional theory for copolymers confined in a nanoslit, *J. Chem. Phys.*, 2007, 126, 134903 (1-6).
- [95] S. Asakura and F. Oosawa, On interaction between two bodies immersed in a solution of macromolecules *J. Chem. Phys.*, 1954, 22, 1255-1256.
- [96] J.L. Barrat and J.P. Hausen, *Basic Concepts for Simple and Complex Liquids*, 2003, Cambridge University Press, Cambridge.
- [97] A. Vrij, Polymers at interfaces and the interactions in colloidal dispersions, *Pure. Appl. Chem.*, 1976, 48, 471-483.
- [98] E.J. Meijer and D. Frenkel, Colloids dispersed in polymer solutions. A computer simulation study, *J. Chem. Phys.*, 1994, 100, 6873-6887.
- [99] W. Poon, Colloids as big atoms, *Science*, 2004. 304, 830-831.
- [100] K.E. Eboigbodin, J.R.A. Newton, A.F. Routh, and C.A. Biggs, Role of nonadsorbing polymers in bacterial aggregation, *Langmuir*, 2005, 21, 12315-12319.
- [101] B. Neu and H.J. Meiselman, Depletion-Mediated Red Blood Cell Aggregation in Polymer Solutions, *Biophys. J.*, 2002, 83, 2482-2490.
- [102] D. Marenduzzo, K. Finan, and P.R. Cook, The depletion attraction: an underappreciated force driving cellular organization, *J. Cell Biol.*, 2006, 175, 681-686.
- [103] A.A. Gorbunov and A.M. Skvortsov, Statistical properties of confined macromolecules, *Adv. Coll. Int. Sci.*, 1995, 62, 31-108.
- [104] I. Teraoka, Polymer solutions in confining geometries, *Prog. Polym. Sci.* 1996, 21, 89-149.
- [105] P. Cifra, T. Bleha and A. Romanov, Monte-Carlo calculations of equilibrium partitioning of flexible chains into pores, *Polymer*, 1988, 29, 1664-1668.

- [106] T. Bleha, P. Cifra, and F.E. Karasz, The effects of concentration on partitioning of flexible chains into pores, *Polymer*, 1990, 31, 1321-1327.
- [107] T. Bleha and F.E. Karasz, Depletion potential between two attractive plates mediated by polymers, *Polymer*, 2005, 46, 10996-11002.
- [108] E. Eisenriegler and R. Maassen, Center-of-mass distribution of a polymer near a repulsive wall, *J. Chem. Phys.*, 2002, 116, 449-450.
- [109] H.-P. Hsu and P. Grassberger, Polymers confined between two parallel plane walls, 2004, 120, 2034-2041.
- [110] S.B. Chen, Monte Carlo simulations of conformations of chain molecules in a cylindrical pore, *J. Chem. Phys.*, 2005, 123, 074702 (1-7).
- [111] J.P. Hernández-Ortiz, H. Ma, J.J. de Pablo, and M.D. Graham, Cross-stream-line migration in confined flowing polymer solutions: Theory and simulation, *J. Chem. Phys.*, 2006, 18, 123101 (1-12).
- [112] J.E. Butler, O.B. Usta, R. Kekre, and A.J.C. Ladd, Kinetic theory of a confined polymer driven by an external force and pressure-driven flow, *Phys. Fluids*, 2007, 19, 113101 (1-14).
- [113] Y. Wang, G.H. Peters, F.Y. Hansen, and O. Hassager, Equilibrium partitioning of macromolecules in confining geometries: Improved universality with a new molecular size parameter, *J. Chem. Phys.*, 2008, 128, 124904 (1-13).
- [114] Y. Wang, G.H. Peters, F.Y. Hansen, and O. Hassager, Proof of the identity between the depletion layer thickness and half the average span for an arbitrary polymer chain, *J. Chem. Phys.*, 2008, 129, 074904 (1-8).
- [115] E.F. Casassa, Distribution of random-flight polymer chains in solution near a barrier, *Macromolecules*, 1984, 17, 601-604.
- [116] E.F. Casassa, Distribution of star-branched random-flight chains in solution near a plane barrier, *Macromolecules*, 1995, 28 (23), pp 7756-7763.
- [117] E.F. Casassa, Distribution of Random-Flight Chains in Solution near Convex Barriers, *Macromolecules*, 1997, 30, 1469-1478.
- [118] D. Kleshchanok, R. Tuinier and P.R. Lang, Direct measurements of polymer-induced forces, *J. Phys.: Condens. Matt.*, 2008, 25, 073101 (1-25).
- [119] A. Sikorski and I. Żukowska, Structure of polymer films in adsorbing slit: A computer simulation study, *Coll. Surf. A*, 2008, 321, 244-248.
- [120] A. Jaeckel and J. Dayantis, Concentration profiles of confined chains having absorbing and reflecting statistics, *Polymer*, 1996, 37, 3447-3449.
- [121] Z. Chen and F.A. Escobedo, Influence of polymer architecture and polymer-wall interaction on the adsorption of polymers into a slit-pore, *Phys. Rev. E*, 2004, 69, 021802 (1-10).
- [122] P. Romiszowski and A. Sikorski, Star-Branched Polymers in an Adsorbing Slit. A Monte Carlo Study, *J. Chem. Phys.*, 2005, 123, 104905.
- [123] P. Romiszowski and A. Sikorski, Dynamics of polymer chains in confined space. A computer simulation study, *Physica A*, 2005, 357, 356-363.
- [124] P. Romiszowski and A. Sikorski, The Structure of star-branched chains in a confined space, *Monatshefte für Chemie*, 2006, 137, 969-976.
- [125] P. Romiszowski and A. Sikorski, The structure of polymer chains in confinement. A Monte Carlo study, *J. Mol. Model.* 2009, 15, 681-686.
- [126] L. He, K.L. Yung, Y. Xu, Y.W. Shen, The effect of surface features on nanorheology of LCP melts in nanochannels by MD Simulation, *J. Tribology*, 2007, 129, 171-176.
- [127] K.L. Yung, L. He, Y. Xu, Y.W. Shen, Study of surface conditions and shear flow of LCP melts in nanochannels through molecular dynamics simulation, *Polymer*, 2006, 47, 4454-4460.

- [128] P.K. Mishra and S. Kumar, Effect of confinement on coil-globule transition, *J. Chem. Phys.*, 2004, 121, 8642-8646.
- [129] P.K. Mishra, D. Giri, S. Kumar, and Y. Singh, Does a surface attached globule phase exist?, *Physica A*, 2003, 318, 171-178.
- [130] R. Rajesh, D. Dhar, D. Giri, S. Kumar, and Y. Singh, Adsorption and collapse transitions in a linear polymer chain near an attractive wall, *Phys. Rev. E*, 2002, 65, 056124 (1-7).
- [131] J.R. Maury-Evertsz, L.A. Estevez, and G.E. Lopez, Equilibrium properties of confined single-chain homopolymers, *J. Chem. Phys.*, 2003, 119, 9925-9932.
- [132] E.H. Feng and G.H. Fredrickson, Confinement of equilibrium polymers: A field-theoretic model and mean-field solution, *Macromolecules*, 2006, 39, 2364-2372.
- [133] K. Jo, D.M. Dhingra, T. Odijk, J.J. de Pablo, M.D. Graham, R. Runnheim, D. Forrest, and D.C. Schwartz, A single-molecule barcoding system using nanoslits for DNA analysis, *Proc. Nat. Acad. Sci. U. S. A.*, 2007, 104, 2673-2678.
- [134] H.P. Huinink, J.C.M. Brokken-Zijp, M.A. van Dijk, G.J.A. Sevink, Asymmetric block copolymers confined in a thin film, *J. Chem. Phys.*, 2000, 112, 2452-2462.
- [135] A. Alexander-Katz, A.G. Moreira and G.H. Fredrickson, Field-theoretic simulations of confined polymer solutions, *J. Chem. Phys.*, 2003, 118, 9030-9036.
- [136] A. Alexander-Katz, A.G. Moreira, S.W. Scotts, and G.H. Fredrickson, Field-theoretic simulations of polymer solutions: Finite-size and discretization effects, *J. Chem. Phys.*, 2005 122, 014904 (1-8).
- [137] K. Shin, H. Xiang, S.I. Moon, T. Kim, T.J. McCarthy, and T.P. Russell, Curving and frustrating flatland, *Science*, 2004, 306, 76.
- [138] H. Xiang, K. Shin, T. Kim, S.I. Moon, T.J. McCarthy, and T.P. Russell, Block copolymers under cylindrical confinement, *Macromolecules*, 2004, 37, 5660-5664.
- [139] D. Cao and J. Wu, Surface-induced phase transitions in ultrathin films of block copolymers, *J. Chem. Phys.*, 2005, 122, 194703 (1-8).
- [140] M. Wang, W. Hu, Y. Ma, and Y.-Q. Ma, Confined crystallization of cylindrical diblock copolymers studied by dynamic Monte Carlo simulations, *J. Chem. Phys.*, 2006, 124, 244901 (1-6).
- [141] P. Maniadis, I.N. Tsimpanogiannis, E.M. Kober and T. Lookman, Phase segregation of diblock copolymers in nanopore geometries, *Europhys. Lett.*, 2008, 81, 56001 (1-6).
- [142] Bin Yu, Pingchuan Sun, Tiehong Chen, Qinghua Jin, Datong Ding, and Baohui Li, Confinement-induced novel morphologies of block copolymers, *Phys. Rev. Lett.*, 2006, 96, 138306 (1-4).
- [143] J.J. Kasianowicz, E. Brandin, D. Branton, and D.W. Deamer, Characterization of individual polynucleotide molecules using a membrane channel, *Proc. Nat. Acad. Sci. U.S.A.*, 1996, 90, 13770-13773.
- [144] A. Meller, L. Nivon, E. Brandin, J. Golovchenko, and D. Branton, Rapid nanopore discrimination between single polynucleotide molecules, *Proc. Nat. Acad. Sci. U.S.A.*, 2000, 97, 1079-1084.
- [145] A. Meller, L. Nivon, E. Brandin, Voltage-driven DNA translocations through a nanopore, *Phys. Rev. Lett.*, 2001, 86, 3435-3438.
- [146] S.E. Henrickson, M. Misakian, B. Robertson, and J.J. Kasianowicz, Driven DNA transport into an asymmetric nanometer-scale pore, *Phys. Rev. Lett.*, 2000, 85, 3057-3060.
- [147] H. Vocks, D. Panja, G.T. Barkema, and R.C. Ball, Pore-blockade times for field-driven polymer translocation, *J. Phys.: Condens. Matt.*, 2008, 20, 095224 (1-8).
- [148] E. Slonkina and B. Kolomeisky, Polymer translocation through a long nanopore, *J. Chem. Phys.*, 2003, 118, 7112-7118.
- [149] Giovanni Maglia, Marcela Rincon Restrepo, Ellina Mikhailova, and Hagan Bayley, Enhanced translocation of single DNA molecules through  $\alpha$ -hemolysin nanopores by manipulation of internal charge, *Proc. Nat. Acad. Sci. U.S.A.*, 2008, 105, 19720-19725.

- [150] T. Hu and B.I. Shklovskii, Theory of DNA translocation through narrow ion channels and nanopores with charged walls, *Phys. Rev. E*, 2008, 78, 032901 (1-3).
- [151] J. Li, M. Gershow, D. Stein, E. Brandin and J.A. Golovchenko, DNA molecules and configurations in a solid-state nanopore microscope, *Nat. Mater.*, 2003, 2, 611-615.
- [152] P. Chen, J.J. Gu, E. Brandin, Y.R. Kim, Q. Wang, and D. Branton, Probing single DNA molecule transport using fabricated nanopores. *Nano Lett.*, 2004, 4, 2293-2298.
- [153] Y. Lansac, P.K. Maiti, and M.A. Glaser, Coarse-grained simulation of polymer translocation through an artificial nanopore, *Polymer*, 2004, 45, 3099-3110.
- [154] R.J. Murphy and M. Muthukumar, Threading synthetic polyelectrolytes through protein pores, *J. Chem. Phys.*, 2007, 126, 051101 (1-4).
- [155] D.K. Lubensky and D.R. Nelson, Driven polymer translocation through a narrow pore, *Biophys. J.*, 1999, 77, 1824-1838.
- [156] M. Muthukumar, Polymer translocation through a hole, *J. Chem. Phys.*, 1999, 111, 10371.
- [157] C.Y. Kong and M. Muthukumar, Modeling of polynucleotide translocation through protein pores and nanotubes, *Electrophoresis*, 2002, 23, 2697-2703.
- [158] M. Muthukumar, Polymer escape through a nanopore, *J. Chem. Phys.*, 2003, 118, 5174-5184.
- [159] Y. Kantor and M. Kardar, Anomalous dynamics of forced translocation, *Phys. Rev. E*, 2004, 69, 021806 (1-12).
- [160] A.J. Storm, C. Storm, J. Chen, H. Zandbergen, J.-F. Joanny, and C. Dekker, Fast DNA translocation through a solid-state nanopore, *Nano Lett.*, 2005, 5, 1193-1197.
- [161] P. Tian and G.D. Smith, Translocation of a polymer chain across a nanopore: A Brownian dynamics simulation study, *J. Chem. Phys.*, 2003, 119, 11475.
- [162] A. Meller and D. Branton, Single molecule measurements of DNA transport through a nanopore, *Electrophoresis*, 2002, 23, 2583.
- [163] J.J. Kasianowicz, S.E. Henrickson, H.H. Weetall, and B. Robertson, Simultaneous Multianalyte Detection with a Nanometer-Scale Pore, *Anal. Chem.*, 2001, 73, 2268.
- [164] O.V. Krasilnikov, C.G. Rodrigues, and S.M. Bezrukov, Single Polymer Molecules in a Protein Nanopore in the Limit of a Strong Polymer-Pore Attraction, *Phys. Rev. Lett.*, 2006, 97, 018301.
- [165] S.M. Iqbal, D. Akin, and R. Bashir, Solid-state nanopore channels with DNA selectivity, *Nat. Nanotech.*, 2007, 2, 243-248.
- [166] H. Yan and B. Xu, Towards rapid DNA sequencing: detecting single-stranded DNA with a solid-state nanopore, *Small*, 2006, 2, 310-312.
- [167] J. Lagerqvist, M. Zwolak, and M. Di Ventra, Fast DNA sequencing via transverse electronic transport, *Nano Lett.*, 2006, 6, 779-782.
- [168] Q. Zhao, G. Sigalov, V. Dimitrov, B. Dorvel, U. Mirsaidov, S. Sligar, A. Aksimentiev, and G. Timp, Detecting SNPs using a synthetic nanopore, *Nano Lett.*, 2007, 7, 1680-1685.
- [169] X. Liang and S.Y. Chou, Nanogap detector inside nanofluidic channel for fast real-time label-free DNA analysis, *Nano Lett.*, 2008, 8, 1472-1476.
- [170] J. Clarke, H.C. Wu, L. Jayasinghe, A. Patel, S. Reid, and H. Bayley, Continuous base identification for single-molecule nanopore DNA sequencing, *Nat. Nanotech.*, 2009, 4, 265-270.
- [171] O.B. Bakajin, T.A.J. Duke, C.F. Chou, S.S. Chan, R.H. Austin, and E.C. Cox, Electrohydrodynamic stretching of DNA in confined environments, *Phys. Rev. Lett.*, 1998, 80, 2737-2740.
- [172] N. Laachi, J. Cho, and K.D. Dorfman, DNA unhooking from a single post as a deterministic process: Insights from translocation modeling, *Phys. Rev. E*, 2009, 79, 031928 (1-9).
- [173] S.W.P. Turner, M. Cabodi, and H.G. Craighead, Confinement-induced entropic recoil of single DNA molecules in a nanofluidic structure, *Phys. Rev. Lett.*, 2002, 88, 128103 (1-4).

- [174] C. Forrey and M. Muthukumar, Langevin dynamics simulations of ds-DNA translocation through synthetic nanopores, *J. Chem. Phys.*, 2007, 127, 015102 (1-10).
- [175] A. Mohan, A.B. Kolomeisky, and M. Pasquali, Effect of charge distribution on the translocation of an inhomogeneously charged polymer through a nanopore, *J. Chem. Phys.*, 2008, 128, 125104 (1-7).
- [176] J. Han and H.G. Craighead, Separation of long DNA molecules in a microfabricated entropic trap array, *Science*, 2000, 288, 1026-1029.
- [177] J. Han and H.G. Craighead, Characterization and optimization of an entropic trap for DNA separation, *Anal. Chem.*, 2002, 74, 394-401.
- [178] Y. Zeng and D.J. Harrison, Confinement effects on electromigration of long DNA molecules in an ordered cavity array, *Electrophoresis*, 2006, 27, 3747-3752.
- [179] Z.R. Li, G.R. Liu, Y.Z. Chen, J.S. Wang, H. Bow, Y. Cheng, and J. Han, Continuum transport model of Ogston sieving in patterned nanofilter arrays for separation of rod-like biomolecules, *Electrophoresis*, 2008, 29, 329-339.
- [180] Z.R. Li, G.R. Liu, J. Han, Y.Z. Chen, J.S. Wang, and N.G. Hadjiconstantinou, Transport of biomolecules in asymmetric nanofilter arrays, *Anal. Bioanal. Chem.*, 2009, 394, 427-435.
- [181] D. Fologea, J. Uplinger, B. Thomas, D.S. McNabb, and J. Li, Slowing DNA translocation in a solid-state nanopore, *Nano Lett.*, 2005, 5, 1734-1737.
- [182] R. Riehn, M. Lu, Y.-M. Wang, S.F. Lim, E.C. Cox, and R.H. Austin, Restriction mapping in nanofluidic devices, *Proc. Nat. Acad. Sci. U. S. A.*, 2005, 102, 10012-10016.
- [183] E.H. Trepagnier, A. Radenovic, D. Sivak, P. Geissler, and J. Liphardt, Controlling DNA capture and propagation through artificial nanopores, *Nano Lett.*, 2007, 7, 2824-2830.
- [184] C.Y. Kong and M. Muthukumar, Simulations of stochastic sensing of proteins, *J. Am. Chem. Soc.*, 2005, 127, 12852-12861.
- [185] S. Kotsev and A.B. Kolomeisky, Effect of orientation in translocation of polymers through nanopores, *J. Chem. Phys.*, 2006, 125, 084906 (1-7).
- [186] R. Randel, H.C. Loebl, and C.C. Matthai, Molecular Dynamics Simulations of polymer translocations, *Macromol. Theor. Simul.*, 2004, 13, 387-391.
- [187] Q. Zhao, J. Comer, V. Dimitrov, S. Yemenicioglu, A. Aksimentiev, and G. Timp, Stretching and unzipping nucleic acid hairpins using a synthetic nanopore, *Nucl. Acid. Res.*, 2008, 1532-1541.
- [188] U. Bockelmann and V. Viasnoff, Theoretical study of sequence-dependent nanopore unzipping of DNA, *Biophys. J.*, 2008, 94, 2716-2724.
- [189] V. Viasnoff, N. Chiaruttini, and U. Bockelmann, Probing DNA base pairing energy profiles using a nanopore, *Euro. Biophys. J.*, 2009, 38, 263-269.
- [190] M. Wanunu, B. Chakrabarti, J. Mathe, D.R. Nelson, and A. Meller, Orientation-dependent interactions of DNA with an alpha-hemolysin channel, *Phys. Rev. E*, 2008, 77, 031904.
- [191] J. Mathe, A. Aksimentiev, D.R. Nelson, K. Schulten, and A. Meller, Orientation discrimination of single-stranded DNA inside the  $\alpha$ -hemolysin membrane channel, *Proc. Nat. Acad. Sci. U. S. A.*, 2005, 102, 12377-12382.
- [192] J.T. Mannion, C.H. Reccius, J.D. Cross, and H.G. Craighead, Conformational analysis of single DNA molecules undergoing entropically induced motion in nanochannels, *Biophys. J.*, 2006, 90, 4538-4545.
- [193] S. Benner, R.J. Chen, N.A. Wilson, R. Abu-Shumays, N. Hurt, K.R. Lieberman, D.W. Deamer, W.B. Dunbar, and M. Akeson, Sequence-specific detection of individual DNA polymerase complexes in real time using a nanopore, *Nat. Nanotech.*, 2007, 2, 718-724.
- [194] C.H. Reccius, S.M. Stavis, J.T. Mannion, L.P. Walker, and H.G. Craighead, Conformation, length, and speed measurements of electrostatically stretched DNA in nanochannels, *Biophys. J.*, 2008, 95, 273-286.

- [195] A.F. Sauer-Budge, J.A. Nyamwanda, D.K. Lubensky, and D. Branton, Unzipping kinetics of double-stranded DNA in a nanopore, *Phys. Rev. Lett.*, 2003, 90, 238101 (1-4).
- [196] J. Mathe, H. Visram, V. Viasnoff, Y. Rabin, and Amit Meller, Nanopore unzipping of individual DNA hairpin molecules, *Biophys. J.*, 2004, 87, 3205-3212.
- [197] J. Mathe, A. Arinstein, Y. Rabin, and Amit Meller, Equilibrium and irreversible unzipping of DNA in a nanopore, *Europhys. Lett.*, 2006, 73, 128-134.
- [198] O.K. Dudko, J. Mathe, A. Szabo, A. Meller, and G. Hummer, Extracting kinetics from single-molecule force spectroscopy: Nanopore unzipping of DNA hairpins, *Biophys. J.*, 2007, 92, 4188-4195.
- [199] O. Dudko, G. Hummer, and A. Szabo, Theory, analysis and interpretation of single-molecule force spectroscopy experiments, 2008 *Proc. Natl. Acad. Sci. U.S.A.*, 105, 15755-760.
- [200] Y. Kafri, D.K. Lubensky, and D.R. Nelson, Dynamics of molecular motors and polymer translocation with sequence heterogeneity, *Biophys. J.*, 2004, 86, 3373-3391.
- [201] U.F. Keyser, B.N. Koeleman, S. van Dorp, D. Krapf, R.M.M. Smeets, S.G. Lemay, N.H. Dekker and C. Dekker, Direct force measurements on DNA in a solid-state nanopore, *Nat. Phys.*, 2006, 2, 473-477.
- [202] C. Dekker, Solid-state nanopores, *Nat. Nanotech.*, 2007, 2, 209-215.
- [203] K. Luo, I. Huopaniemi, T. Ala-Nissila, and S.-C. Ying, Polymer translocation through a nanopore under an applied external field, *J. Chem. Phys.*, 2006, 124, 114704 (1-7).
- [204] I. Huopaniemi, K. Luo, T. Ala-Nissila, and S.-C. Ying, Langevin dynamics simulations of polymer translocation through nanopores, *J. Chem. Phys.*, 2006, 125, 124901 (1-8).
- [205] J.L.A. Dubbeldam, A. Milchev, V.G. Rostiashvili, and T. A. Vilgis, Driven polymer translocation through a nanopore: A manifestation of anomalous diffusion, *Europhys. Lett.*, 2007, 79, 18002 (1-6).
- [206] D. Panja and G.T. Barkema, Passage times for polymer translocation pulled through a narrow pore, *Biophys. J.*, 2008, 94, 1630-1637.
- [207] H.C. Loebel, R. Randel, S.P. Goodwin, and C.C. Matthai, Simulation studies of polymer translocation through a channel, *Phys. Rev. E*, 2003, 67, 041913 (1-5).
- [208] K. Luo, T. Ala-Nissila, S.-C. Ying, and A. Bhattacharya, Heteropolymer translocation through nanopores, *J. Chem. Phys.*, 2007, 126, 145101 (1-7).
- [209] K. Luo, T. Ala-Nissila, S.-C. Ying, and A. Bhattacharya, Influence of polymer-pore interactions on translocation, *Phys. Rev. Lett.*, 2007, 99, 148102 (1-4).
- [210] K. Luo, T. Ala-Nissila, S.-C. Ying, and A. Bhattacharya, Dynamics of DNA translocation through an attractive nanopore, *Phys. Rev. E*, 2008, 78, 061911 (1-6).
- [211] W. Sung and P.J. Park, Polymer Translocation through a Pore in a Membrane, *Phys. Rev. Lett.*, 1996, 77, 783-786.
- [212] M. Muthukumar, Polymer translocation through a hole, *J. Chem. Phys.*, 1999, 111, 10371-10374.
- [213] Y.-C. Chen, C. Wang, and M.-B. Luo, Simulation study on the translocation of polymer chains through nanopores, *J. Chem. Phys.*, 2007, 127, 044904 (1-6).
- [214] Y. Xie, H. Yang, H. Yu, Q. Shi, X. Wang, and J. Chen, Excluded volume effect on confined polymer translocation through a short nanochannel, *J. Chem. Phys.*, 2006, 124, 174906 (1-4).
- [215] M.-B. Luo, Translocation of polymer chains through interacting nanopores, *Polymer*, 2007, 48, 7679-7686.
- [216] P. J. Park and W. Sung, Polymer translocation induced by adsorption, *J. Chem. Phys.*, 1998, 108, 3013-3018.
- [217] A. Milchev, K. Binder, and A. Bhattacharya, Polymer translocation through a nanopore induced by adsorption: Monte Carlo simulation of a coarse-grained model, *J. Chem. Phys.*, 2004, 121, 6042-6051.

- [218] J.K. Wolterink, G.T. Barkema, and D. Panja, Passage Times for Unbiased Polymer Translocation through a Narrow Pore, *Phys. Rev. Lett.*, 2006, 96, 208301.
- [219] D. Panja, G.T. Barkema, and R.C. Ball, Anomalous dynamics of unbiased polymer translocation through a narrow pore, *J. Phys.: Condens. Matt.*, 2007, 19, 432202 (1-8).
- [220] D. Panja, G. T. Barkema, and R. C. Ball, Polymer translocation out of planar confinements, *J. Phys.: Condens. Matt.*, 2008, 20, 075101 (1-9).
- [221] J.L.A. Dubbeldam, A. Milchev, V.G. Rostiashvili, and T.A. Vilgis, Polymer translocation through a nanopore: A showcase of anomalous diffusion, *Phys. Rev. E*, 2007, 76, 010801 (R) (1-4).
- [222] K. Luo, T. Ala-Nissila, and S.-C. Ying, Polymer translocation through a nanopore: A two-dimensional Monte Carlo study, *J. Chem. Phys.*, 2006, 124, 034714 (1-5).
- [223] S. Guillouzie and G.W. Slater, Polymer translocation in the presence of excluded volume and explicit hydrodynamic interactions *Phys. Lett. A*, 2006, 359, 261-264.
- [224] R. Gasparac, D.T. Mitchell and C.R. Martin, Electrokinetic DNA transport in a nanopore membrane, *Electrochim. Acta*, 2004, 49, 847-850.
- [225] S. Ghosal, Electrophoresis of a polyelectrolyte through a nanopore, *Phys. Rev. E*, 2006, 74, 041901 (1-5).
- [226] S. Ghosal, Effect of Salt Concentration on the Electrophoretic Speed of a Polyelectrolyte through a Nanopore, *Phys. Rev. Lett.*, 2007, 98, 238104 (1-4).
- [227] S. Ghosal, Electrokinetic-flow-induced viscous drag on a tethered DNA inside a nanopore, *Phys. Rev. E*, 2007, 061916 (1-3).
- [228] C.T.A. Wong and M. Muthukumar, Polymer capture by electro-osmotic flow of oppositely charged nanopores, *J. Chem. Phys.*, 2007, 126, 164903 (1-6).
- [229] S. Pennathur, F. Baldessari, J.G. Santiago, M.G. Kattah, J.B. Steinman, and P.J. Utz, Free-Solution Oligonucleotide Separation in Nanoscale Channels, *Anal. Chem.*, 2007, 79, 8316-8322.
- [230] X. Liang, K.J. Morton, R.H. Austin, and S.Y. Chou, Single Sub-20 nm Wide, Centimeter-Long Nanofluidic Channel Fabricated by Novel Nanoimprint Mold Fabrication and Direct Imprinting, *Nano Lett.*, 2007, 7, 3774-3780.
- [231] B. Luan and A. Aleksei, Electro-osmotic screening of the DNA charge in a nanopore, *Phys. Rev. E*, 2008, 78, 021912.
- [232] S. van Dorp, U.F. Keyser, N.H. Dekker, C. Dekker, S.G. Lemay, Origin of the electrophoretic force on DNA in solid-state nanopores, *Nat. Phys.*, 2009, 5, 347-351.
- [233] M.A. Webster and J.M. Yeomans, Modeling a tethered polymer in Poiseuille flow, *J. Chem. Phys.*, 2005, 122, 164903 (1-6).
- [234] D. Stein, F.H.J. van der Heyden, W.J.A. Koopmans, and C. Dekker, Pressure-driven transport of confined DNA polymers in fluidic channels, *Proc. Nat. Acad. Sci. U. S. A.*, 2006, 103, 15853-15858.
- [235] J. Zhang, J.S. Hansen, B.D. Todd, and P.J. Davis, Structural and dynamical properties for confined polymers undergoing planar Poiseuille flow, *J. Chem. Phys.*, 2007, 126, 144907 (1-14).
- [236] R.B. Schoch, L.F. Cheow, and J. Han, Electrical detection of fast reaction kinetics in nanochannels with an induced flow, *Nano Lett.*, 2007, 7, 3895-3900.
- [237] P. Abgrall and N.T. Nguyen, Nanofluidic Devices and Their Applications, *Anal. Chem.*, 2008, 80, 2326-2341.
- [238] Y.-D. He, H.-J. Qian, Z.-Y. Lu, and Z.-S. Li, Polymer translocation through a nanopore in mesoscopic simulations, *Polymer*, 2007, 48, 3601-3606.
- [239] G.M. Wang and W.C. Sandberg, Non-equilibrium all-atom molecular dynamics simulations of free and tethered DNA molecules in nanochannel shear flows, *Nanotech.*, 2007, 18, 135702 (1-9).

- [240] W.C. Sandberg and G.M. Wang, Atomic hydrodynamics of DNA: Coil-uncoil-coil transitions in a wall-bounded shear flow, *Phys. Rev. E*, 2008, 78, 061910 (1-12).
- [241] S.C. Kohale and R. Khare, Cross stream chain migration in nanofluidic channels: Effects of chain length, channel height, and chain concentration, *J. Chem. Phys.*, 2009, 130, 104904 (1-8).
- [242] K.-G. Wang, S. Yue, L. Wang, A. Jin, C. Gu, P.-Ye Wang, Y. Feng, Y. Wang, and H. Niu, Manipulating DNA molecules in nanofluidic channels, *Microfluid. Nanofluid.*, 2006, 2, 85-88.
- [243] K. Wang, S. Yue, L. Wang, A. Jin, C. Gu, P. Wang, H. Wang, X. Xu, Y. Wang, and H. Niu, Nanofluidic channels fabrication and manipulation of DNA molecules, *IEE Proc.-Nanobiotechnol.*, 2006, 153, 11-15.
- [244] H.T. Hoang, I.M. Segers-Nolten, J.W. Berenschot, M.J. de Boer, N.R. Tas, J. Haneveld, and M.C. Elwenspoek, Fabrication and interfacing of nanochannel devices for single-molecule studies, *J. Micromech. Microeng.*, 2009, 19, 065017 (1-10).